โครงการ

การเรียนการสอนเพื่อเสริมประสบการณ์

ชื่อโครงการ การศึกษาการดูดซับและการสลายตัวของไนโตรซามีนบนสารประกอบคาร์บอน, โบรอนไนไตรด์, เบอริลเลียมออกไซด์และอะลูมิเนียมฟอสไฟด์ที่มีโครงสร้างคล้ายกรงแบบโซดาไลท์ด้วยวิธีดีเอฟที

DFT investigation on adsorption of nitrosamine on C_{24}, $B_{12}N_{12}$, $Be_{12}O_{12}$ and $Al_{12}P_{12}$ sodalite-like cage and their decomposition mechanism

ชื่อนิสิต นางสาวมนรดา เพชรมาก **เลขประจำตัว** 5833073423

ภาควิชา เคมี

ปีการศึกษา 2561

คณะวิทยาศาสตร์ จุฬาลงกรณ์มหาวิทยาลัย

บทคัดย่อและแฟ้มข้อมูลฉบับเต็มของโครงงานทางวิชาการที่เปิดให้บริการในคลังปัญญาจุฬาฯ (CUIR)
เป็นแฟ้มข้อมูลของนิสิตเจ้าของโครงงานทางวิชาการที่ส่งผ่านทางคณะที่สังกัด
The abstract and full text of senior projects in Chulalongkorn University Intellectual Repository(CUIR)
are the senior project authors' files submitted through the faculty.

การศึกษาการดูดซับและการสลายตัวของไนโตรซามีนบนสารประกอบคาร์บอน, โบรอนไนไตรด์, เบอริลเลียมออกไซด์และอะลูมิเนียมฟอสไฟด์ที่มีโครงสร้างคล้ายกรงแบบโซดาไลท์ด้วยวิธีดีเอฟที

โดย

นางสาวมนรดา เพชรมาก

รายงานนี้เป็นส่วนหนึ่งของการศึกษาตามหลักสูตร

ปริญญาวิทยาศาสตรบัณฑิต

ภาควิชาเคมี คณะวิทยาศาสตร์

จุฬาลงกรณ์มหาวิทยาลัย

ปีการศึกษา 2561

DFT investigation on adsorption of nitrosamine on C_{24}, $B_{12}N_{12}$, $Be_{12}O_{12}$ and $Al_{12}P_{12}$ sodalite-like cage and their decomposition mechanism

Miss Monrada Petchmark

In Partial Fulfilment for the Degree of Bachelor of Science

Department of Chemistry, Faculty of Science
Chulalongkorn University

Academic Year 2018

Project Title: DFT investigation on adsorption of nitrosamine on C_{24}, $B_{12}N_{12}$, $Be_{12}O_{12}$, and $Al_{12}P_{12}$ sodalite-like cage and their decomposition mechanism

Student name: Ms. Monrada Petchmark

Field of study: Chemistry

Project Advisor: Professor Dr. Vithaya Ruangpornvisuti

Accept by Department of Chemistry, Faculty of Science, Chulalongkorn University in Partial Fulfillment of the Requirement for the Degree of Bachelor of Science.

.....Head of Department of Chemistry

(Associate Professor Vudhichai Parasuk, Ph.D.)

PROJECT COMMITTEE

.....Chair Committee

(Associate Professor Buncha Pulpoka, Ph.D.)

.....Project Advisor

(Professor Vithaya Ruangpornvisuti, Dr.rer.nat.)

.....Committee

(Associate Professor Viwat Vchirawongkwin, Dr. rer. nat.)

ชื่อโครงการ การศึกษาการดูดซับและการสลายตัวของไนโตรซามีนบนสารประกอบคาร์บอน, โบรอนไนไตรด์, เบอริลเลียมออกไซด์และอะลูมิเนียมฟอสไฟด์ที่มีโครงสร้างคล้ายกรงแบบโซดาไลท์ด้วยวิธีดีเอฟที

ชื่อนิสิตในโครงการ นางสาวมนรดา เพชรมาก เลขประจำตัว 5833073423

ชื่ออาจารย์ที่ปรึกษา ศาสตราจารย์ ดร.วิทยา เรืองพรวิสุทธิ์

ภาควิชาเคมี คณะวิทยาศาสตร์ จุฬาลงกรณ์มหาวิทยาลัย ปีการศึกษา 2561

บทคัดย่อ

โครงสร้างที่เหมาะสมของการดูดซับแก๊สไนโตรซามีนคอนฟอร์เมอร์บนสารประกอบคาร์บอน (CSL, C_{24}), โบรอนไนไตรด์ (BNSL, $B_{12}N_{12}$), เบอริลเลียมออกไซด์ (BeOSL, $Be_{12}O_{12}$) และอะลูมิเนียมฟอสไฟด์ (AlPSL, $Al_{12}P_{12}$) ที่มีโครงสร้างคล้ายกรงแบบโซดาไลท์ ได้รับการศึกษาโดยใช้วิธีการคำนวณด้วยทฤษฎีเดนซิตีฟังก์ชันนอล DFT/CAM-B3LYP/6-31+G(d,p) ผลการคำนวณให้ค่าทางเทอร์โมไดนามิกส์ของการดูดซับระหว่างแก๊สไนโตรซามีนกับสารประกอบที่มีโครงสร้างคล้ายกรงแบบโซดาไลท์ได้แก่ พลังงานการดูดซับ การเปลี่ยนแปลงเอนทัลปี และการเปลี่ยนแปลงพลังงานอิสระกิบส์ และได้ศึกษากลไกการสลายตัวของแก๊สไนโตรซามีนบนสารประกอบที่มีโครงสร้างคล้ายกรงแบบโซดาไลท์จากวิธีการคำนวณข้างต้น พบว่าไนโตรซามีนสามารถสลายตัวบนสารประกอบที่มีโครงสร้างคล้ายกรงแบบโซดาไลท์ได้ดีโดยได้ผลิตภัณฑ์เป็นแก๊สไนโตรเจนและน้ำ ซึ่งทำให้เกิดปฏิกิริยาการสลายตัวบนคาร์บอนที่มีโครงสร้างคล้ายกรงแบบโซดาไลท์เป็นปฏิกิริยาทางเดียวและมี 3 ขั้นตอน สำหรับปฏิกิริยาการสลายตัวของไนโตรซามีนบนสารประกอบโบรอนไนไตรด์ เบอริลเลียมออกไซด์ และอะลูมิเนียมฟอสไฟด์ที่มีโครงสร้างคล้ายกรงแบบโซดาไลท์เป็นปฏิกิริยาที่มี 2 ขั้นตอน โดยขั้นแรกคือขั้นตอนการดูดซับแก๊สและขั้นตอนที่สองคือขั้นตอนการสลายตัวของไนโตรซามีนสารประกอบที่มีโครงสร้างคล้ายกรงแบบโซดาไลท์ทั้ง 4 ชนิดนี้สามารถเป็นตัวเร่งปฏิกิริยาในปฏิกิริยาการเปลี่ยนแก๊สไนโตรซามีนซึ่งเป็นแก๊สพิษ เป็นแก๊สที่ไม่มีพิษคือแก๊สไนโตรเจนและน้ำได้ โดยความสามารถในการเร่งปฏิกิริยาของสารประกอบที่มีโครงสร้างคล้ายกรงแบบโซดาไลท์จากน้อยไปมากเป็นดังนี้ AlPSL > BeOSL >> BNSL > CSL

คำสำคัญ: คาร์บอน; โบรอนไนไตรด์; เบอริลเลียมออกไซด์; อะลูมิเนียมฟอสไฟด์; โครงสร้างคล้ายกรงแบบโซดาไลท์; การดูดซับไนโตรซามีน; การเปลี่ยนเป็นแก๊สไนโตรเจนและน้ำ; ทฤษฎีเดนซิตีฟังก์ชันนอล

Project Tile: DFT investigation on adsorption of nitrosamine on C_{24}, $B_{12}N_{12}$, $Be_{12}O_{12}$ and $Al_{12}P_{12}$ sodalite-like cage and their decomposition mechanism

Student Name: Ms. Monrada Petchmark Student ID 5833073423

Advisor Name: Professor Dr. Vithaya Ruangpornvisuti

Department of Chemistry, Faculty of Science, Chulalongkorn University, Academic Year 2018

Abstract

Structure optimizations for adsorption configurations of nitrosamine conformers on sodalite-like cages of carbon (CSL, C_{24}), boron nitride (BNSL, $B_{12}N_{12}$), beryllium oxide (BeOSL, $Be_{12}O_{12}$) and aluminium phosphide (AlPSL, $Al_{12}P_{12}$) were carried out using the density functional theory (DFT) method with CAM–B3LYP level of theory. Energetics, enthalpies and Gibbs free energies of adsorptions of nitrosamine conformers were obtained. Reaction mechanisms of nitrosamine conformer conversion to N_2 and H_2O on the CSL, BNSL, BeOSL and AlPSL cages, and their energetic profiles were obtained. The nitrosamine conversion to N_2 and H_2O on the CSL cage, three step reaction was found. Reaction mechanisms of nitrosamine conversion to N_2 and H_2O on the BNSL, BeOSL and AlPSL cages are two step reaction which the first and second steps are adsorption and conversion steps, respectively. All the nanocages, CSL, BNSL, BeOSL and AlPSL can be used as catalysts in the conversion reaction of nitrosamine (toxic gas) to N_2 and H_2O (non–toxic gases) and their catalytic performances are in order: AlPSL > BeOSL >> BNSL > CSL.

Keywords Carbon; boron nitride; beryllium oxide; aluminum phosphide; Sodalite-like cages; nitrosamine adsorption; conversion to nitrogen and water; DFT method

ACKNOWLEDGEMENTS

I would like to sincerely thank my advisor Professor Dr. Vithaya Ruangpornvisuti for his useful guidance, encouragement and critiques throughout the course of this study. Without his guidance and instruction, this study would not be achievable. I was so appreciated with his opportunity that provided me to be able to join the study under his instruction with kindness and valuable guidance.

Furthermore, I would like to thank to my committee: Associate Professor Dr. Buncha Pulpoka and Associate Professor Dr. Viwat Vchirawongkwin who review, comment and suggest on this work.

A special thanks to my seniors in VR lab who encouraged and gave me tips to get the work successful. Thank you for your support and encouragement throughout this work. I will not get this far without their help.

My thanks also go out to my friends who encouraged me when I'm so tired and give the good advice to me during working this study.

Last but not least, I would like to heartfelt thank my parents who are important in my life. Thank you for always believing in me and giving all support to study in undergraduate study life. So with due regards, I express my gratitude to them

Miss Monrada Petchmark

CONTENTS

LIST OF FIGURES

LIST OF TABLES

CHAPTER I

INTRODUCTION

1.1 Background and Literature review

Nitrosamine ($ONNH_2$) is a toxic gas that is classified by the International Agency for Research on Cancer (IARC) as the cancer risk for humans [1]. The nitrosamine occurs as contaminants in various categories of foods and beverages [2, 3], drinking water [3], beer [4] and many kinds of foods. Foods such as cheese, both fresh and salted fish were most extensively and occasionally found to contain traces of nitrosamines [5]. Researches of exploring on materials for nitrosamine elimination and catalysts for conversion of nitrosamine to non–toxic gases have been hardly found. The synthesized novel hollow molecularly imprinted polymer (HMIPs) microspheres as adsorption *N*–nitrosamines were investigated [6]. Materials, such as mesoporous molecular sieve SBA–15 [7], zeolites H–ZSM–5 [7-10], Li–ZSM–5 [9, 10], Na–ZSM–5 [9, 10] and SWCNTs [11] on adsorption of nitrosamines were studied for non–catalytic purpose. Decomposition of *N*–nitrosamine on zeolites Y and ZSM–5 was studied [12] but decomposition mechanism has not been shown. As nanocages have been widely investigated, several types of nanocages as toxic gas storage and catalysts for conversion of toxic gas to non–toxic gas have been extensively studied.

The smallest fullerene cages for C, BN, BeO and AlP compounds which compose of 24 atoms are sodalite-like cages and their formulae are C_{24}, $B_{12}N_{12}$, $Be_{12}O_{12}$ and $Al_{12}P_{12}$, respectively which are here noted as CSL, BNSL, BeOSL and AlPSL cages, respectively. The CSL (C_{24}) was studied on adsorption of benzene [13], hydrogen [14]and 5–Fluorouracil drug [15] and properties of symmetrical structure [16] and stability [17]. BNSL nanocage involved with geometry [18], electronic structure [19], its fluorinated species [20], adsorptions of carbon dioxide [21], adenine, uracil, and cytosine [19], ozone [22], lithium atom and ion [23] and interaction with graphene and boron nitride nanosheets [24] was studied. The BeOSL nanocage was investigated for hydrogen adsorption for storage purpose [25] and acetone adsorption [26]. Recently, adsorptions of lithium atom and ion [23] and HCOH and H_2S molecules on AlPSL cage was theoretically studied using DFT method [27].

In previous studies, nine conformers of nitrosamine in gas phase were found, and one amino (*a*–nsm) conformer and three imino (*i*–nsm) conformers were found to be the most and the second most stable conformers, respectively [28], these two types of nitrosamine conformers have been employed as adsorbate gas. This study has investigated the adsorption of nitrosamine (toxic gas) on four different sodalite-like cages, CSL, BNSL, BeOSL and AlPSL cages which high potentials are expected, as gas storage materials and their catalytic properties.

1.2 Theoretical background

Quantum chemistry applies quantum mechanics to calculate properties of molecule that can figure out the problem in chemistry. The three main quantum mechanic methods to calculated molecular properties are *ab initio*, semi-empirical and the density-functional methods. These methods based on quantum mechanical principle to predict and explain chemical behavior. Quantum chemical calculation relates to ground state of individual atom and molecule, transition state and excitation state that occur throughout the chemical reaction.

1.2.1 *Ab Initio* method[29]

Ab initio calculations are computational method based on quantum chemistry solving Schrödinger equation,

$$H\psi = E\psi \tag{1.1}$$

where $\hat{H}$ is Hamiltonian operator, E is the total energy of the system and ψ is the n-electron wave function, respectively. The kinetic and potential energies for each of the particles were indicated by Hamiltonian operator ($\hat{H}$) which are explained in the equation (1.2).

$$H = -\frac{\hbar^2}{2m_e}\sum_{i}^{electrons}\nabla_i^2 - \frac{\hbar^2}{2}\sum_{A}^{nuclei}\frac{1}{M_A}\nabla_A^2 - \frac{e^2}{4\pi\varepsilon_0}\sum_{i}^{electrons}\sum_{A}^{nuclei}\frac{Z_A}{r_{iA}}$$
$$+\frac{e^2}{4\pi\varepsilon_0}\sum_{i>}^{electrons}\sum_{j}^{electrons}\frac{1}{r_{ij}} + \frac{e^2}{4\pi\varepsilon_0}\sum_{A>}^{nuclei}\sum_{B}^{nuclei}\frac{Z_A Z_B}{R_{AB}} \quad (1.2)$$

where Z is the nuclear charge, m_e is the mass of electron, R_{AB} is distance between nuclei A and B, r_{ij} is distance between electrons i and j, r_{iA} is distance between electrons i and nucleus A and ε_0 is the permittivity of vacuum[30].

Because there is not solution for many-electron system, the Hartree-Fock method (HF) is the starting point of *ab initio* method. The Hartree-Fock method is the simplest approach of *ab initio* method that the instantaneous coulombic electron-electron repulsion is not specially considered. Only its average effect is included in this calculation.

In many-electron system, linear combination of atomic orbitals (LCAO) which all atomic orbitals are combined is applied to represent ψ. The possible approximate polyelectronic wavefunction as product of one-electron wavefunctions is written in equation

$$\psi_0 = \psi_0(1)\psi_0(2)\psi_0(3)...\psi_0(n) \quad (1.3)$$

The function ψ_0 relies on the coordinates of all electrons in atom, $\psi_0(n)$ is a function of the n electron in atom which can be expanded by basis set. Because the HF nonlinearities approximation, the Self-consistent-field-procedure (SCF) is method that is used to solve the HF equation. The SCF cycles are continuously calculated until self-consistency is achieved. The spin orbitals and configuration state functions can be constructed by HF equation. Electrons in the system can move independently in a mean field potential because the Hartree-Fock method ignores electron correlation in the system. It is hard to perform the accurate calculations with large basis sets containing many atoms and electrons. Additionally, wavefunction cannot measure observable feature of molecule or atom. Therefore, the density functional theory (DFT) method becomes popular method to calculate in chemical system simulation.

1.2.2 Density functional theory (DFT) method[31]

Density functional theory (DFT) method is based on the electron probability density function, called simply the electron density or charge density, and designated by $\rho(x, y, z)$ which is related to the "component" one-electron spatial wavefunctions Ψ_i (the molecular orbitals) of a single-determinant wavefunction Ψ by equation

$$\rho = \sum_{i=1}^{n} n_i \left|\Psi_i\right|^2 \tag{1.4}$$

1.2.2.1 The Kohn-Sham equations[32]

From the wavefunction theory, the Hartree-Fock variational approach led to the Hartree-Fock equations which are used to calculate energy and the wavefunction. However, the Kohn-Sham equations which are the basis of current molecular DFT calculations have variational approach that might yield a way to calculate the energy and electron density. There are two ideas in Kohn-Sham method consist of (1) to express the molecular energy as a sum of terms, only one of which, a relatively small term. As a result, even moderately large errors in this term will not introduce large errors into the total energy. And (2) to use an initial guess of the electron density ρ in the Kohn-Sham equations to calculate an initial guess of the Kohn-Sham orbitals and energy levels. Then, this initial guess used to iteratively refine these orbitals and energy levels. The final Kohn-Sham orbitals are used to calculate electron density that can be used to calculate the energy of molecule. The electron density distribution of the reference system, which is by order the same as that of the ground state of our real system is given by

$$\rho_0 = \rho_r = \sum_{i=1}^{2n} \left|\psi_i^{KS}(1)\right|^2 \tag{1.5}$$

where the ψ_i^{KS} are the Kohn-Sham spatial orbitals. Substituting the above expression for the electron density in term of orbitals into the energy and varying E_0 relating to the ψ_i^{KS} which leads to the Kohn-Sham equation

$$\left[-\frac{1}{2}\nabla_i^2 - \sum_{nucleiA} \frac{Z_A}{\mathbf{r}_{1A}} + \int \frac{\rho(\mathbf{r}_2)}{r_{12}} d\mathbf{r}_2 + v_{XC}(1)\right]\psi_i^{KS}(1) = \varepsilon_i^{KS}\psi_i^{KS}(1) \tag{1.6}$$

where ε_i^{KS} is the Kohn-Sham energy level and $v_{XC}(1)$ is the exchange correlation potential. The expression in bracket is the Kohn-Sham operator, $\hat{h}^{KS}$. Because the Kohn-Sham equations are a set of one-electron equation with the subscript i running from 1 to $2n$, over all the electrons in the system, they random installed electron number one in the Kohn-Sham orbitals and the exchange correlation potential. The exchange correlation potential v_{XC} obtained from the exchange-correlation energy E_{XC} which is a functional of $\rho(\mathbf{r})$ and the process to obtain v_{XC} is described as

$$v_{xc}(\mathbf{r}) = \frac{\delta E_{XC}\left[\rho(\mathbf{r})\right]}{\delta\rho(\mathbf{r})} \tag{1.7}$$

The differentiation of exchange correlation potential v_{XC} is shown as being with respect to $\rho(\mathbf{r})$, but $\rho(\mathbf{r})$ is explained in terms of Kohn-Sham orbitals. The Kohn-Sham equation can be defined by

$$h^{KS}(1)\psi_i^{KS}(1) = \varepsilon_i^{KS}\psi_i^{KS}(1) \tag{1.8}$$

In Kohn-Sham system, the energy also compensates for self-repulsion in charge cloud of ρ.and for the deviation of the kinetic energy of noninteracting Kohn-Sham electrons from that of real electrons. For this reason, we should have the good functional handles that not only exchange correlation errors, but also self-repulson and kinetic errors. The hybrid functional is the choice to improve calculations.

1.2.2.2 The Hybrid functionals[29]

The hybrid exchange correlation functionals increase the density functional energy. The popular hybrid functional is B3LYP which is hybrid GGA functional. GGA functional is defined by

$$E_{xc}^{GGA}\left[\rho^{\alpha},\rho^{\beta}\right] = \int f\left(\rho^{\alpha}(\mathbf{r}),\rho^{\beta}(\mathbf{r}),\nabla\rho^{\alpha}(\mathbf{r}),\nabla\rho^{\beta}(\mathbf{r})\right)d\mathbf{r} \tag{1.9}$$

where f are some functions of spin densities and their gradient. The letter GGA stands for generalized-gradient approximation. This functional is developed using theoretical considerations.

Often some empiricism is thrown in by choosing the values of parameters in the functional to show good performance for known values of molecular properties.

The hybrid GGA called B3LYP is defined by

$$E_{xc}^{B3LYP} = (1 - a_0 - a_x)E_x^{LSDA} + a_0 E_x^{HF} + a_x E_x^{B88} + (1 - a_c)E_x^{VWN} + a_c E_c^{LYP} \tag{1.10}$$

where E_x^{HF} is the Kohn-Sham orbitals based on HF exchange energy functional. E_x^{LSDA} is the kind accurate pure DFT, the local-spin-density approximation which is non-gradient-corrected exchange functional.

$$E_x^{LSDA} = -\frac{3}{4}\left(\frac{6}{\pi}\right)^{1/3} \int \left[\left(\rho^{\alpha}\right)^{4/3} + \left(\rho^{\beta}\right)^{4/3} \right] d\mathbf{r} \tag{1.11}$$

E_x^{B88} is the Beck 88 exchange functional.

$$E_x^{B88} = E_x^{LSDA} + \Delta E_x^{B88} \tag{1.12}$$

$$\Delta E_x^{B88} = -\beta \rho^{1/3} \frac{x^2}{1 + 6\beta x \sinh^{-1} x} \tag{1.13}$$

where β parameter is determined by fitting to known atomic data and x is dimension gradient variable.

The E_x^{VWN} is the Vosko, Wilk, Nusair function is defined by

$$E_x^{VWN} = E_x^{LSDA}(1 + ax^2 + bx^4 + cx^6)^{1/5} \tag{1.14}$$

$$x = \frac{|\nabla \rho|}{\rho^{4/3}} \tag{1.15}$$

The E_x^{VWN} forms part of the perfect functional for the homogenous electron of the LDA and LSDA. E_c^{LYP} is the LYP correlation functional. The parameters a_0, a_x and a_c give good fit to experimental molecular atomization energies.

1.2.3 Gaussian basis set[30]

Basis sets that made up of a finite number of well-defined functions centered of each atom are required in the linear combination of atomic orbitals (LCAO) approximation. Those functions would be corresponding closely to the exact solution of hydrogen atom. Nevertheless, the use of these functions was not cost effective, and early numerical calculations were implemented using nodeless Slater-type orbitals (STOs) which defined by

$$\phi(r,\theta,\phi) = \frac{(2\zeta / a_0)^{n+1/2}}{\left[(2n)!\right]^{1/2}} r^{n-1} e^{-\zeta r/a_0} Y_l^m(\theta,\phi)\beta \tag{1.16}$$

Here, *n, m,* and *l* denote the usual quantum number and ζ is the effective nuclear charge. The Slater functions was popular in the years immediately but soon deserted because they lead to integrals that are difficult if not impossible to evaluate analytically. The cost of calculations can be reduced if the AOs are expanded in terms of Gaussian functions which are in form

$$g_{ijk}(r) = Nx^i y^j z^k e^{-\alpha r^2} \tag{1.17}$$

In this equation, *x, y*, and *z* are the position coordinates measured from the nucleus of an atom; *i, j*, and *k* are non-negative integers that the sum of these values determines the types of orbitals, and α is an orbital exponent. Gaussian functions lead to integrals that are easily evaluated. Except for semi-empirical models, which do not actually entail evaluation of large number of difficult integrals, all practical quantum chemical models now make use of Gaussian functions.

The different radial dependence of STOs and Gaussian function, first, the Gaussian functions are appropriate choices for AOs. The solution to this problem is to approximate the STO by a linear combination of Gaussian function having different α values, rather than by a single Gaussian function. Using more Gaussian functions can improve cloud electrons to fit well in AOs.

In practice, instead of taking individual Gaussian functions as members of basis set, a normalized linear combination of Gaussian functions with fixed coefficients give the value that is optimized either by searching minimum atom energies or by comparing calculated and experimental results for representative molecule. These linear combinations are called contracted functions that become the elements of the basis set. The coefficients are variable.

1.2.3.1 Minimal Basis set

The minimal basis sets have one and only one basis function defined for each type of orbital core through valence. There are two types of minimal basis sets which are Slater type orbitals (STO) and Gaussian type orbital (GTO). The most widely used and extensively documented is the STO-3G basis set. Each of the basis functions is expanded in terms of three Gaussian functions, where the values of the Gaussian exponents and the linear coefficients have been determined by least squares as best fits to Slater-type (exponential) functions. There are two obvious deficiency in the minimal basis sets: the first is that basis sets can be described atom with spherical molecular environments or nearly spherical molecular environments better than atoms with aspherical environments. So, this basis set will be biased in favor of those incorporating the most spherical atoms. The second deficiency is that basis functions are atom centered. As a result, this basis cannot describe electron distribution between nuclei, which are a critical element of chemical bond.

1.2.3.2 Split-Valence Basis sets

The split-valence basis set correspond to core atomic orbitals by one set of functions and valence atomic orbitals by two sets of functions, $1s$, $2s^i$, $2p_x^i$, $2p_y^i$, $2p_z^i$, $2s^o$, $2p_x^o$, $2p_y^o$, $2p_z^o$ for lithium to neon and $1s$, $2s$, $2p_x$, $2p_y$, $2p_z$, $3s^i$, $3p_x^i$, $3p_y^i$, $3p_z^i$, $3s^o$, $3p_x^o$, $3p_y^o$, $3p_z^o$ for sodium to argon. Note that the valence $2s$ ($3s$) functions are also split into inner, ^{i} and outer,^{o} components, and that hydrogen atoms are also represented by inner and outer valence ($1s$) functions. There are many types of split-valence basis sets, but the simplest basis sets are 3-21G and 6-31G.

1.2.3.3 Polarization Basis sets

The second deficiency of a minimal basis sets that basis functions are centered on atom rather than between atoms can be improve by the inclusion of polarization functions. The inclusion of polarization functions can be thought about either in term of hybrid orbitals. The term arises from the fact that d functions permit the electron distribution to be polarized (displaced along a particular direction). Polarization functions enable the SCF process to establish a more anisotropic electron distribution than would otherwise be possible. The simplest polarization basis set is 6-31G* which formed from 6-31G by adding a set of *d*-type polarization functions written in term of a single Gaussian for each heavy atom. Polarization functions have chosen Gaussian exponents to give the

lowest energies for representative molecules. However, the polarization basis function does not stand for initial atomic orbital (IAO) which is useful to analyses obtained atomic orbitals and molecular orbitals because, the basis function of p orbital is combined to s orbital, and the basis function of d orbital is combined to p orbital in many cases.

1.2.3.4 Diffuse Basis sets

The highest energy electrons for molecules in calculations involving anions such as absolute acidity calculations and calculations of molecules in excited states may only be associated with specific atoms (or pairs of atoms) loosely. Because, in highest spin state, electrons are assigned in more outer shell orbital where electron is unoccupied in lowest spin state. The diffuse basis functions can supplement for increase accuracy in specific calculations. For example, diffuse *s*- and *p*-type functions, on heavy (non-hydrogen) atoms (designated with a plus sign as in 6-31+G* and 6-31+G**). It may also desirable to provide hydrogens with diffuse *s*-type functions (designated by two plus signs as in 6-31++G* and 6-31++G**).

1.2.4 Thermodynamics properties[33]

Reaction thermodynamics can be explained by quantum chemical calculations which are combining the energies of reactant and product molecules. The basic equations used to describe thermochemical quantities consist of enthalpy, Gibbs free energy and rate of reaction.[33]

1.2.4.1 Enthalpies and Gibbs free energies of reaction

The typical procedure to calculate enthalpies of reaction is to calculate heats of formation, and take the appropriate sums and difference which can be described in equation:

$$\Delta_r H^o(298K) = \sum_{products} {}_f H^o_{prod}(298K) - \sum_{reactants} \Delta_f H^o_{react}(298K) \qquad (1.18)$$

Nonetheless, since Gaussian provides the sum of electronic and thermal enthalpies, there is a short cut. This works since the number of atoms of each element is the same on both sides of the

reaction, therefore all the atomic information cancels out, and the calculations need only the molecular data. The enthalpies of reaction can be calculated simply by

$$\Delta_r H^o(298K) = \sum(\varepsilon_0 + H_{corr})_{products} - \sum(\varepsilon_0 + H_{corr})_{reactants} \tag{1.19}$$

where ε_0 is the total electronic energy and H_{corr} is the correction to the enthalpy due to internal energy which can be described in equation:

$$H_{corr} = E_{tot} + k_B T \tag{1.20}$$

where k_B and T are the Boltzmann constant and temperature which default is 298.15 K, respectively. E_{tot} is the total internal energy which can be describe in equation:

$$E_{tot} = E_t + E_r + E_v + E_e \tag{1.21}$$

where E_t, E_r, E_v and E_e are the internal energy due to translation, rotational motion, vibrational motion and electronic motion, respectively. Likewise to the short cut in enthalpies, Gibbs free energies of reaction can be calculated in form

$$\Delta_r G^o(298K) = \sum(\varepsilon_0 + G_{corr})_{products} - \sum(\varepsilon_0 + G_{corr})_{reactants} \tag{1.22}$$

where G_{corr} is the correction to the Gibbs free energy due to internal energy which can be calculated by

$$G_{corr} = H_{corr} - TS_{tot} \tag{1.23}$$

where S_{tot} is the total entropy which can be describes in form

$$S_{tot} = S_t + S_r + S_v + S_e \tag{1.24}$$

Note that S_t, S_r, S_v and S_e are entropy due to translation, rotational motion, vibrational motion and electronic motion.

1.2.4.2 Rates of reaction

Rates of reaction can be calculated by equation

$$k(T) = \frac{k_B T}{hc^o} e^{-\Delta^{\ddagger} G^o / RT} \tag{1.25}$$

where k_B, T, R, h and c^o are the Boltzmann constant, absolute temperature, gas constant, the Plank constant and concentration which c^o = 1, respectively. $-\Delta^{\ddagger} G^o$ is the free energy of activation. More complex reactions will need more sophisticated analyses, perhaps including careful determination of the effects of low frequency modes on the transition state and tunneling effects.

1.2.5 NBO analysis

Natural bond orbitals analysis (NBO) is developed as a technique for studying hybridization and covalency effects in polyatomic wavefunctions, based on local block eigenvectors of the one-particle density matrix. [34] NBO analysis use the natural orbitals instead of the molecular orbitals directly. Natural orbitals are the eigenfunctions of the first-order reduced density matrix that are then localized and orthogonalized. The localization procedure allows orbitals to be defined as those centered on atoms and those encompassing pairs of atoms. These can be integrated to obtain charges on the atoms. This results in a population analysis scheme that is less basis set dependent than the Mulliken scheme. However, basis set effects are still readily apparent. NBO analysis is a popular technique because it is available in many software packages and researchers find it convenient to use a method that classifies the type of orbitals.[35]

1.3 Objectives

In this study, the adsorption energies, the thermodynamic properties and charge transfer from various active sites of nitrosamine adsorbed on CSL, BNSL, BeOSL and AlPSL cages with all possible configurations have been studied. Also, the conversion reactions of nitrosamine which is toxic gas to water and nitrogen molecules which are non–toxic gases on CSL, BNSL, BeOSL and AlPSL cages have been investigated.

CHAPTER II

COMPUTATIONAL DETAILS

2.1 Structure optimization

Full optimizations of adsorption structures of nitrosamine on CSL(C_{24}), BNSL ($B_{12}N_{12}$), BeOSL ($Be_{12}O_{12}$) and AlPSL ($Al_{12}P_{12}$) cages, nitrosamine conformers (four most stable conformers), related adsorption structures, corresponding transition–state structures and all related molecules were carried out using density functional theory (DFT) method. DFT calculations have been performed with the CAM–B3LYP method [36] which is the long–range–corrected version of hybrid density functional B3LYP, the Becke's three–parameter exchange functional [37] with the Lee–Yang–Parr correlation functional [38], using the Coulomb–attenuating method and the 6–31+G(d,p) basis set [39] was selected. The frequency calculations using the CAM–B3LYP /6–31+G(d,p) level of theory and NBO charges of all atoms were obtained by NBO population analysis at the same theory. Transition state for reaction paths were investigated as mentioned in ref. [40]. All calculations were performed with the GAUSSIAN 09 program [41].

2.2 Definitions of reaction terms

2.2.1 Adsorption of nitrosamines conformers on sodalite-like cage

The adsorption energies (ΔE_{ads}) for nitrosamine conformers (gas) adsorbed on the CSL, BNSL, BeOSL and AlPSL cages have been obtained using Equation (2.1).

$$\Delta E_{ads}\,(\text{gas}) = E(\text{gas/cage}) - [E(\text{cage}) + E(\text{gas})] \qquad (2.1)$$

where E(nsm/cage) is total energy of nitrosamine (nsm) gas adsorbed on cage, CSL, BNSL, BeOSL or AlPSL. E(nsm) and E(cage) are total energies of isolated nitrosamine conformer and cage, respectively.

2.2.2 Thermodynamic quantities

The standard enthalpy ΔH^{o}_{298} [42] and Gibbs free energy changes ΔG^{o}_{298} of reactions of nitrosamine on CSL(C_{24}), BNSL ($B_{12}N_{12}$), BeOSL ($Be_{12}O_{12}$) and AlPSL ($Al_{12}P_{12}$) cages have been derived from the frequency calculations [43] at the CAM–B3LYP /6–31+G(d,p) level of theory. The rate constants $k(T)$ at temperature T, based on transition state theory, were evaluated from the activation energy, $\Delta^{\ddagger}E$ using Equation (2.2).

$$k(T) = \kappa \frac{k_{\mathrm{B}}T}{h} \frac{Q_{\mathrm{TS}}}{Q_{\mathrm{REA}}} \exp(\frac{-\Delta^{\ddagger}E}{RT}) \tag{2.2}$$

where κ is the tunneling coefficient of which value can be evaluated using the Wigner method [44, 45] with $\kappa = 1 + \frac{1}{24}(\frac{h\nu_i}{k_{\mathrm{B}}T})$, where ν_i is the imaginary frequency that accounts for the vibration motion along the reaction path. k_{B}, h and R are the Boltzmann's constant, Plank's constant and gas constant, respectively. Q_{TS} and Q_{REA} are the partition functions of the transition state and its corresponding reactant, respectively. These partition functions defined as the product of translational, rotational, vibrational and electronic partition functions of species were obtained from their frequency calculations. The equilibrium constant K at 298.15 K (K_{298}) and 1 atm is computed using a thermodynamic equation, $K_{298} = \exp(\frac{-\Delta G^{o}_{298}}{R \times 298.15})$.

2.3 The electric conductivity

The electric conductivity (σ) is a function of energy gap (E_{g}) [46] as shown in Equation (2.3).

$$\sigma = A\, exp\left(\frac{-E_g}{2k_BT}\right) \tag{2.3}$$

where A is the pre–exponential constant. As the energy–gap change (ΔE_{g}) is a difference between energies of the adsorption–state ($E_{\mathrm{g}}^{\mathrm{ads}}$) and clean nano–cage ($E_{\mathrm{g}}^{\mathrm{clean}}$), relation between electric conductivity of the adsorption–state (σ_{ads}) and clean nano–cage (σ_{clean}) can therefore be written in term of $\sigma_{ads}/\sigma_{clean}$ ration as shown in Equation (2.4).

$$\frac{\sigma_{ads}}{\sigma_{clean}} = \frac{-\Delta E_g}{2k_B T} \tag{2.4}$$

As the negative value of ΔE_g gives a positive value of the $\sigma_{ads}/\sigma_{clean}$ ratio, the electric conductivity of the adsorption–state of nano-cage must be raised.

CHAPTER III

RESULTS AND DISCUSSIONS

The CAM–B3LYP/6–31+G(d,p)–optimized structures of cages CSL, BNSL, BeOSL and AlPSL are shown in Figure 3.1. The four conformers of nitrosamine in gas phase, one amino conformer (*a*–nsm) and three imino conformers (*i*–nsm–W, *i*–nsm–9° and *i*–nsm–9^N) were found as shown in Figure 3.1. The stabilities of four nitrosamine conformers are in order: *a*–nsm > *i*–nsm–9^N > *i*–nsm–9° > *i*–nsm–W which correspond with previous work [28]. Adsorption structures of amino and imino types nitrosamine conformers are denoted by *a*–nsm and *i*–nsm, respectively.

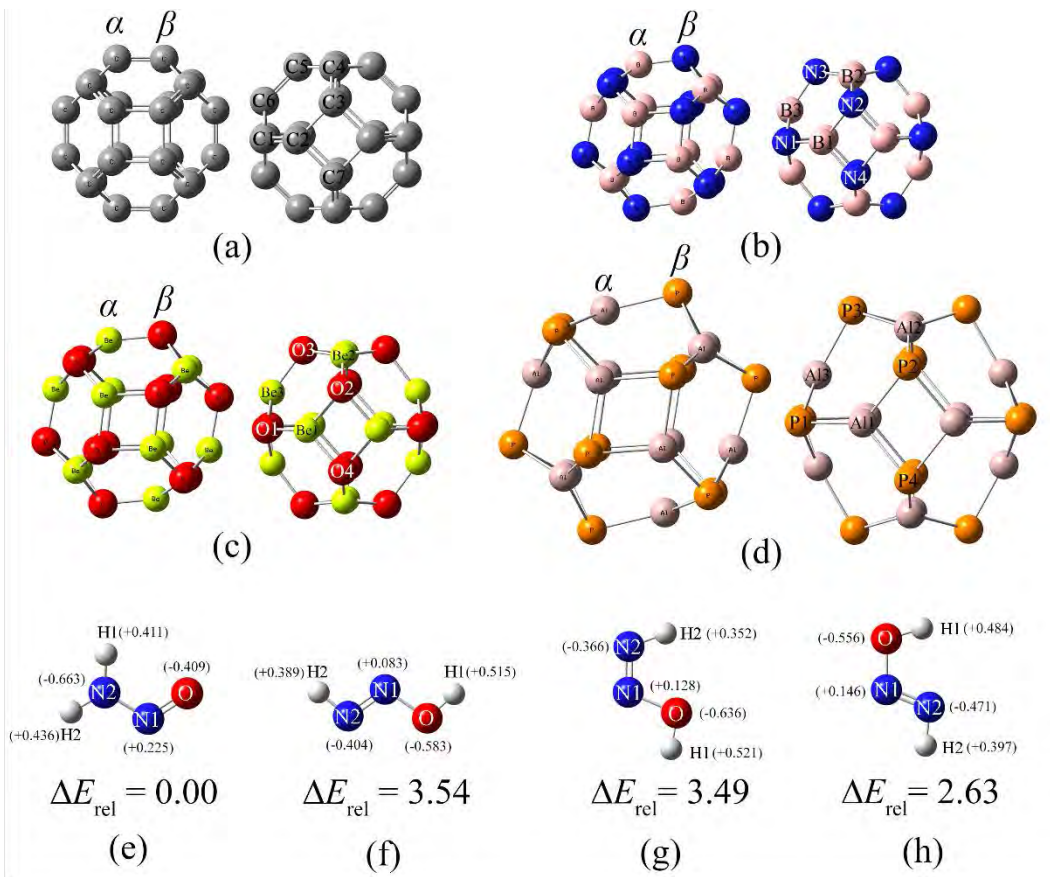

Figure 3.1 The CAM-B3LYP/6-31+G(d,p)–optimized structures of (a) CSL, (b) BNSL, (c) BeOSL and (d) AlPSL cages. The right views show their labelled atoms. The optimized structures of nitrosamine as (e) amino, *a*-nsm, (f) *i*-nsm-W, (g) *i*-nsm-9° and (h) *i*-nsm-9^N conformers of which relative energies (ΔE_{rel}) are shown in kcal/mol.

3.1 Adsorption and reaction on the CSL cage

Adsorption structures of nitrosamine conformers on the CSL cage including *a*–nsm/CSL–1, *a*–nsm/CSL–2, *i*–nsm/CSL–1, *i*–nsm/CSL–2 and *i*–nsm/CSL–3 are shown in Figure 3.2. Also, the shortest bond–distances between atom(s) of nitrosamine conformers and surface atom(s) of the CSL are shown in Figure 3.2. The *a*–nsm/CSL–2 and *i*–nsm/CSL–3 conformers that are respectively single and double interaction modes and show long hydrogen–bond distances are the physical adsorption. The *a*–nsm/CSL–1 is only configuration of dissociative chemisorption. Configurations of *i*–nsm/CSL–1 and *i*–nsm/CSL–2 are non–dissociative chemisorption and their *i*–nsm conformers are slightly different. Adsorption ability is in order: *a*–nsm/CSL–1 > *i*–nsm/CSL–1 > *i*–nsm/CSL–2 > *a*–nsm/CSL–2 > *i*–nsm/CSL–3. The *a*–nsm/CSL–1 is dissociative chemisorption but *i*–nsm/CSL–1 and *i*–nsm/CSL–2 are non–dissociative chemisorption.

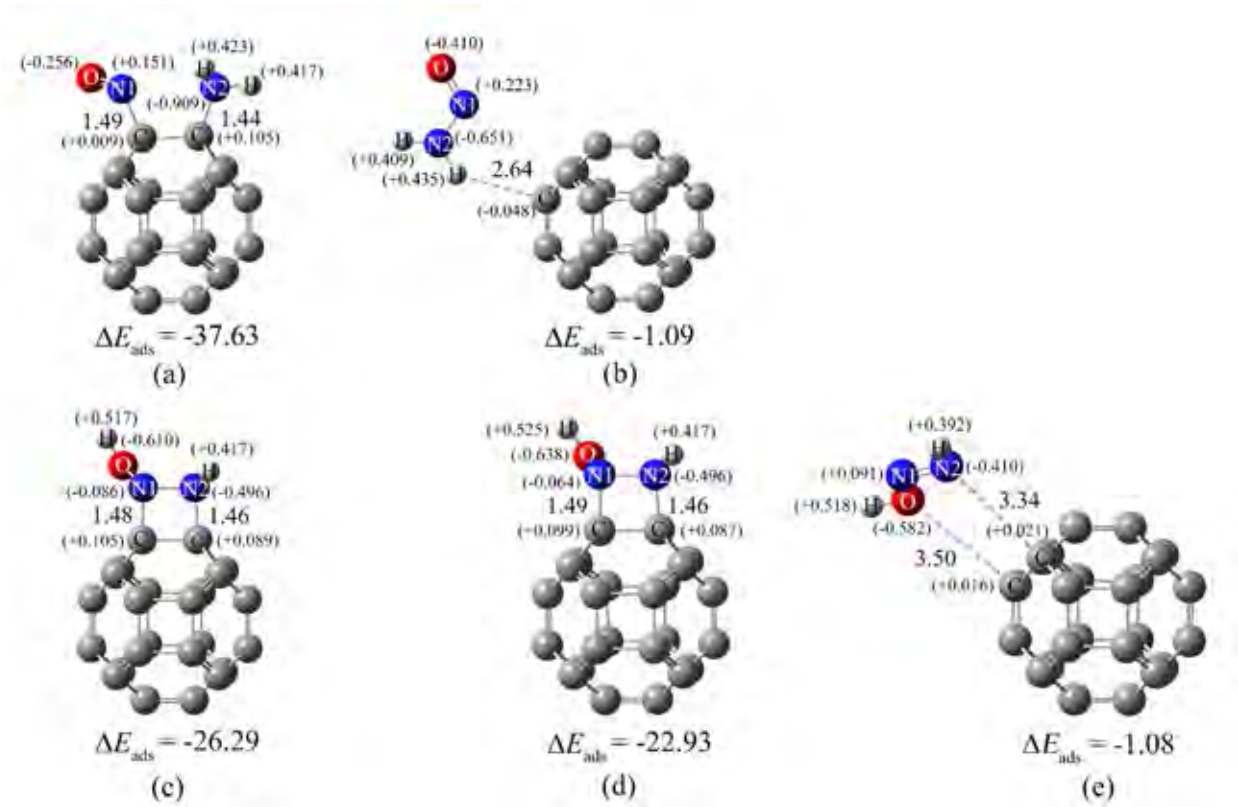

Figure 3.2 The CAM-B3LYP/6-31+G(d,p)–optimized structures of adsorption configurations of (a) *a*-nsm/CSL-1, (b) *a*-nsm/CSL-2, (c) *i*-nsm/CSL-1, (d) *i*-nsm/CSL-2 and (e) *i*-nsm/CSL-3. Adsorption energies are in kcal/mol and bond distances are in Å.

All the adsorption configurations are exothermic processes as shown in Table 3.1. The *a*–nsm/CSL–2 (ΔE_{ads}= –1.09 kcal/mol) and *i*–nsm/CSL–3 (ΔE_{ads}= –1.08 kcal/mol) are physisorption with very weak adsorption and non–spontaneous process. Energy gaps, adsorption energies and thermodynamic quantities of nitrosamine conformers adsorbed on the CSL are shown in Table 3.1.

Table 3.1 Energy gaps, adsorption energies and thermodynamic quantities of nitrosamine conformers of CSL nanocages.

Configuration	E_g [a]	ΔE_g [b]	ΔE_{ads} [c]	ΔH^o_{ads} [d]	ΔG^o_{ads} [d]
CSL:	4.95	–	–	–	–
a–nsm/CSL–1	4.79	–3.29	–37.63	–38.17	–24.80
a–nsm/CSL–2	4.90	–0.99	–1.09	–0.87	7.94
i–nsm/CSL–1	4.82	–2.57	–26.29	–27.14	–13.08
i–nsm/CSL–2	4.83	–2.41	–22.93	–23.78	–9.80
i–nsm/CSL–3	4.95	–0.09	–1.08	–0.74	7.16

[a] In eV.

[b] Percentage of energy–gap change compared with clean nanocage.

[c] Based on zero–point energy correction, in kcal/mol.

[d] At 298.15 K, in kcal/mol.

The negative value of ΔE_g of the *a*–nsm/CSL–1 indicates that CSL adsorption *a*–nsm to form *a*–nsm/CSL–1 configuration results highest change in electric conductivity (ΔE_g= –3.29%) but it is still low. The *i*–nsm/CSL–2 (ΔE_{ads}= –22.93 kcal/mol) is an only configuration that *i*–nsm (see Figure 3.2) can be converted to water and nitrogen molecules.

NBO atomic charges of nitrosamine conformers, atoms nearby adsorption area of the CSL cage and partial charge transfer (PCT) of bonded atoms of the cage are shown in Table 3.2. Binding sites of nanocages, based on bonded atoms defined as $\boldsymbol{\alpha}$ and $\boldsymbol{\beta}$ atoms which are ($\boldsymbol{\alpha} = \boldsymbol{\beta}$ = C atom) or CSL as shown in Figure 3.2. PCTs on the *a*–nsm/CSL–1, *i*–nsm/CSL–1 and *i*–nsm/CSL–2 configurations show that electrons of C1 and C2 of the CSL transfer to nitrosamine resulting strong adsorption. PCTs on the *a*–nsm/CSL–2 show that electron of amino hydrogen transfers to C1 of the CSL but electron of C2 transfers to adjacent C atoms. For the *i*–nsm/CSL–3, electrons of hydroxyl–oxygen and imino–nitrogen atoms slightly transfer to C1 and C2 of the CSL cage, respectively. Nevertheless, the *i*–nsm/CSL–3 is formed with very weak interaction energy. PCTs

of ***α*** and ***β*** of the *a*–nsm/CSL–2 the *i*–nsm/CSL–3 are low because of their weak interactions, see Table 3.2.

Table 3.2 NBO atomic charges of nitrosamine conformers, atoms nearby adsorption area of the CSL nanocages and partial charge transfer (PCT) of bonded atoms of nanocages.

Configuration	NBO partial charge [a]							PCT [d]	
	Nitrosamine atoms [b]					Nanocages [c]			
	O	**N1**	**N2**	**H1**	**H2**	***α***	***β***	***α***	***β***
Clean CSL	–	–	–	–	–	0.044	–0.019	–	–
a–nsm/CSL–1	–0.256	0.151	–0.909	0.423	0.417	0.105	0.009	0.061	0.028
a–nsm/CSL–2	–0.410	0.223	–0.651	0.435	0.409	0.015	0.008	–0.029	0.027
i–nsm/CSL–1	–0.610	–0.086	–0.496	0.417	0.517	0.105	0.089	0.061	0.108
i–nsm/CSL–2	-0.638	-0.064	-0.496	0.417	0.525	0.099	0.087	0.055	0.106
i–nsm/CSL–3	–0.582	0.091	–0.410	0.392	0.518	0.018	–0.020	–0.026	–0.001

[a] In e.

[b] Atoms of nitrosamine conformers defined in Figure 3.1.

[c] Atoms of bonded atom(s) (***α*** and ***β***) of nanocages which are (***α*** = ***β*** = C atom) for CSL cages, as shown in Figure 3.1.

[d] Partial charge transfer, defined as a charge difference between adsorption–site atoms (***α*** and ***β***) of adsorption and non–adsorption states, in e.

As the *i*–nsm/CSL–2 was found to be adsorption intermediate for conversion of nitrosamine conformer to N_2 and water, the *i*–nsm/CSL–2 is thus the starting configuration for conversion of *i*–nsm–9° isomer to water and nitrogen molecules. Energy profile of nitrosamine (*i*–nsm–9° isomer) conversion to water and nitrogen molecules on the CSL cage as shown Figure 3.3. Detail of related structure in Figure 3.3 are shown in Figure 3.4.

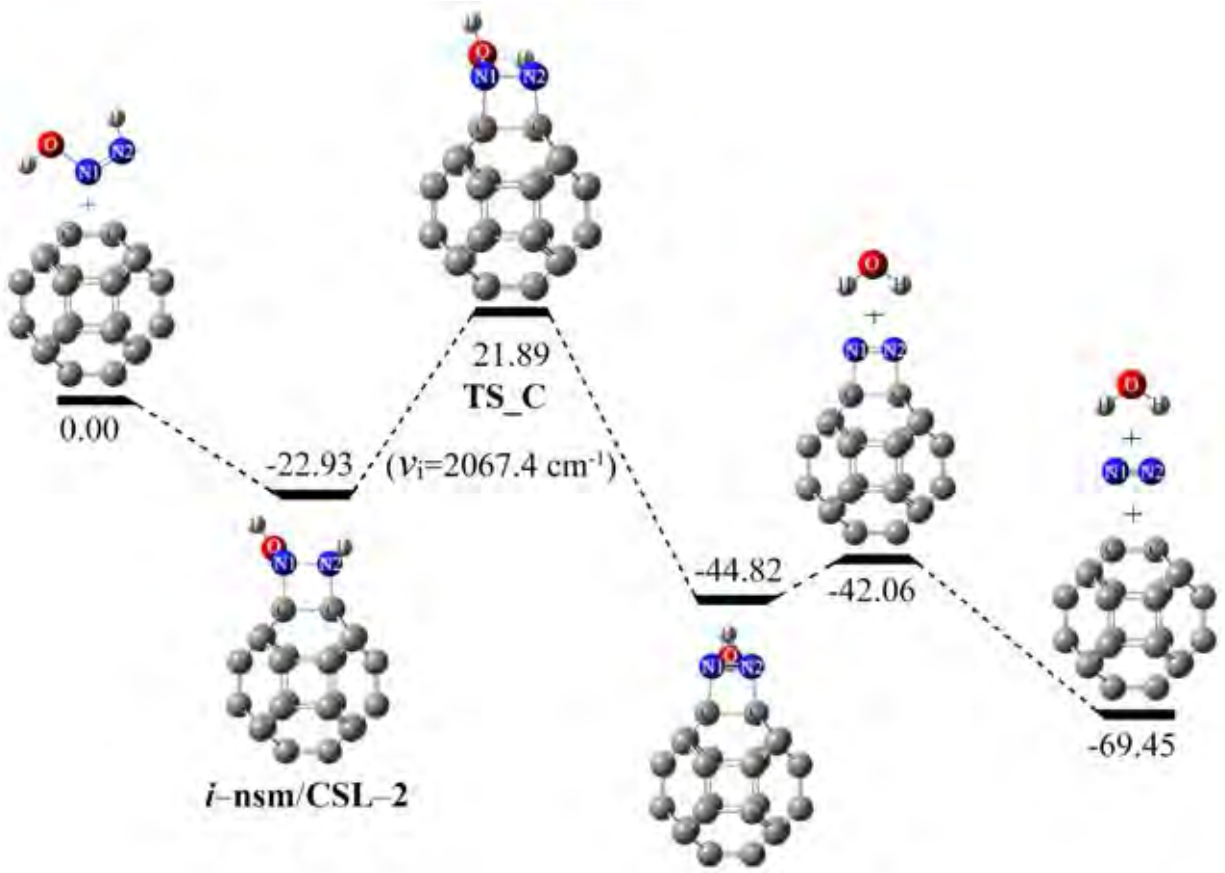

Figure 3.3 Potential energy profile of nitrosamine conversion to water and nitrogen molecules on the CSL cage. The relative energies are in kcal/mol.

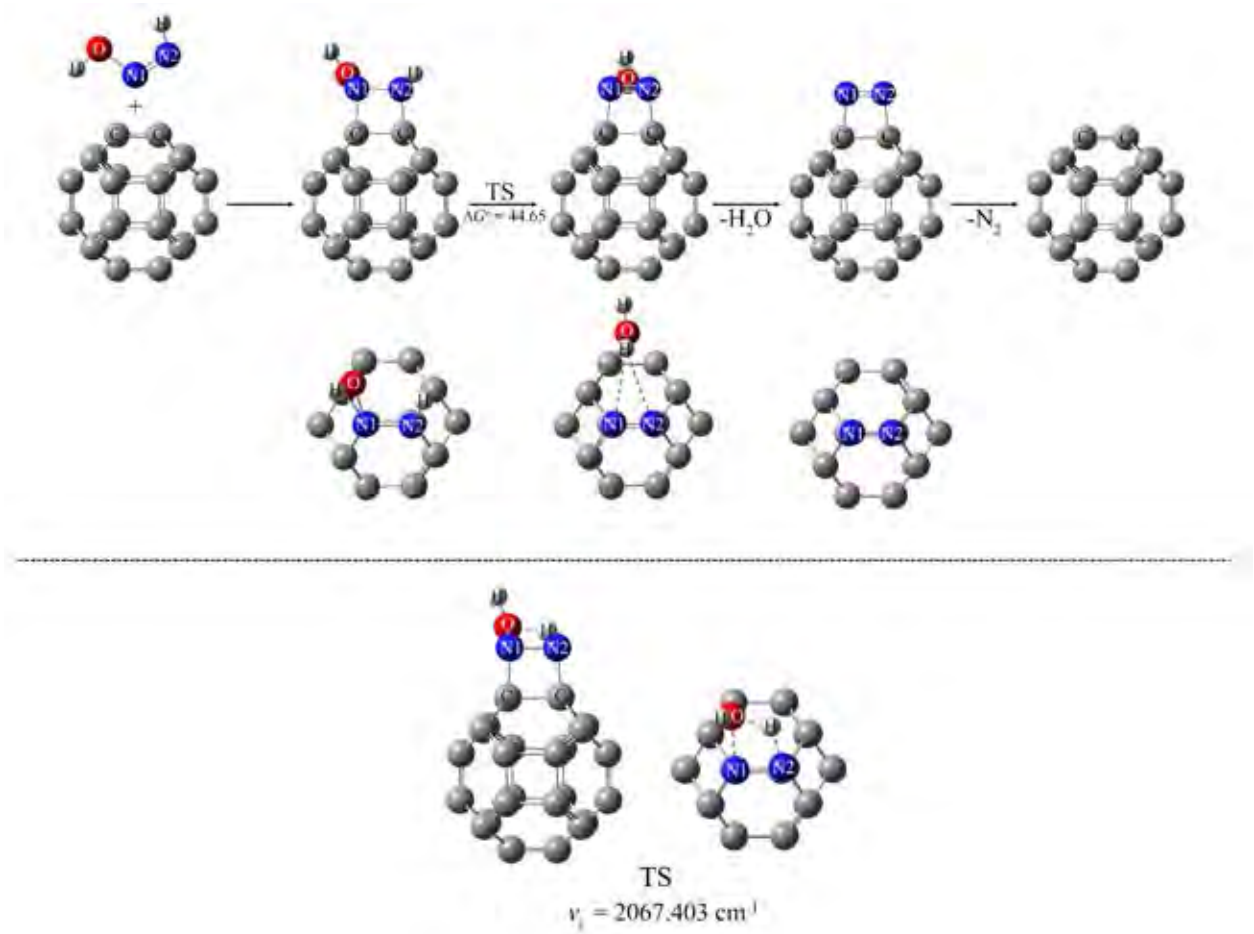

Figure 3.4 Mechanism of nitrosamine conversion to water and nitrogen molecules on the CSL cage. Their top views are located below. The transition-state structure (TS) of which side and top views are respectively at left and right sides, is shown at the bottom.

The first step is adsorption of *i*–nsm on the CSL cage of which adsorption energy is –22.93 kcal/mol. The next step is rate determining step via transition state (TS_C) with activation energy of 44.81 kcal/mol. The transition–state structure of TS_C is confirmed with single–imaginary frequency of ν_i = 2067.4 cm^{-1}. The third step is desorption of water molecule with energy change of 2.76 kcal/mol. The last step is desorption of nitrogen molecule which is the energetic preferred reaction (ΔE_{react} =–27.39 kcal/mol). All the steps of conversion reaction are spontaneous processes as show in Table 3.3.

Table 3.3 Thermodynamic quantities, rate constant and equilibrium constants of reaction steps of conversion of nitrosamine to water and nitrogen molecules on the CSL cage.

Reaction step	$\Delta^{\ddagger}E$ [a]	$\Delta^{\ddagger}G$ [b]	k_{298} [c]	ΔE [d]	ΔH^{o}_{298} [d]	ΔG^{o}_{298} [d]	K_{298}
i–nsm+CSL–2 → *i*–nsm/CSL–2	–	–	–	–22.93	–23.78	–9.80	1.54×10^{7}
i–nsm/CSL–2 → **TS_C** → H_2O/N_2/CSL	44.81	44.65	1.16×10^{20}	–44.82	–43.99	–34.88	3.73×10^{25}
H_2O/N_2/CSL → $H_2O + N_2$/CSL	–	–	–	2.76	2.36	–3.86	6.81×10^{2}
N_2/CSL → N_2 + /CSL	–	–	–	–27.39	–26.06	–38.21	1.02×10^{28}

[a] Activation energy, in kcal/mol.

[b] Gibbs free energy at activation, in kcal/mol.

[c] In s^{-1}.

[d] In kcal/mol.

3.2 Adsorption and reaction on BNSL cage

The CAM–B3LYP/6–31+G(d,p)–optimized structure of the BNSL cage is shown in Figure 3.1. Adsorption structures of amino and imino nitrosamine conformers are shown in Figure 3.5 and Figure 3.6, respectively. All adsorption structures of amino and imino nitrosamine conformers are five and nine configurations respectively.

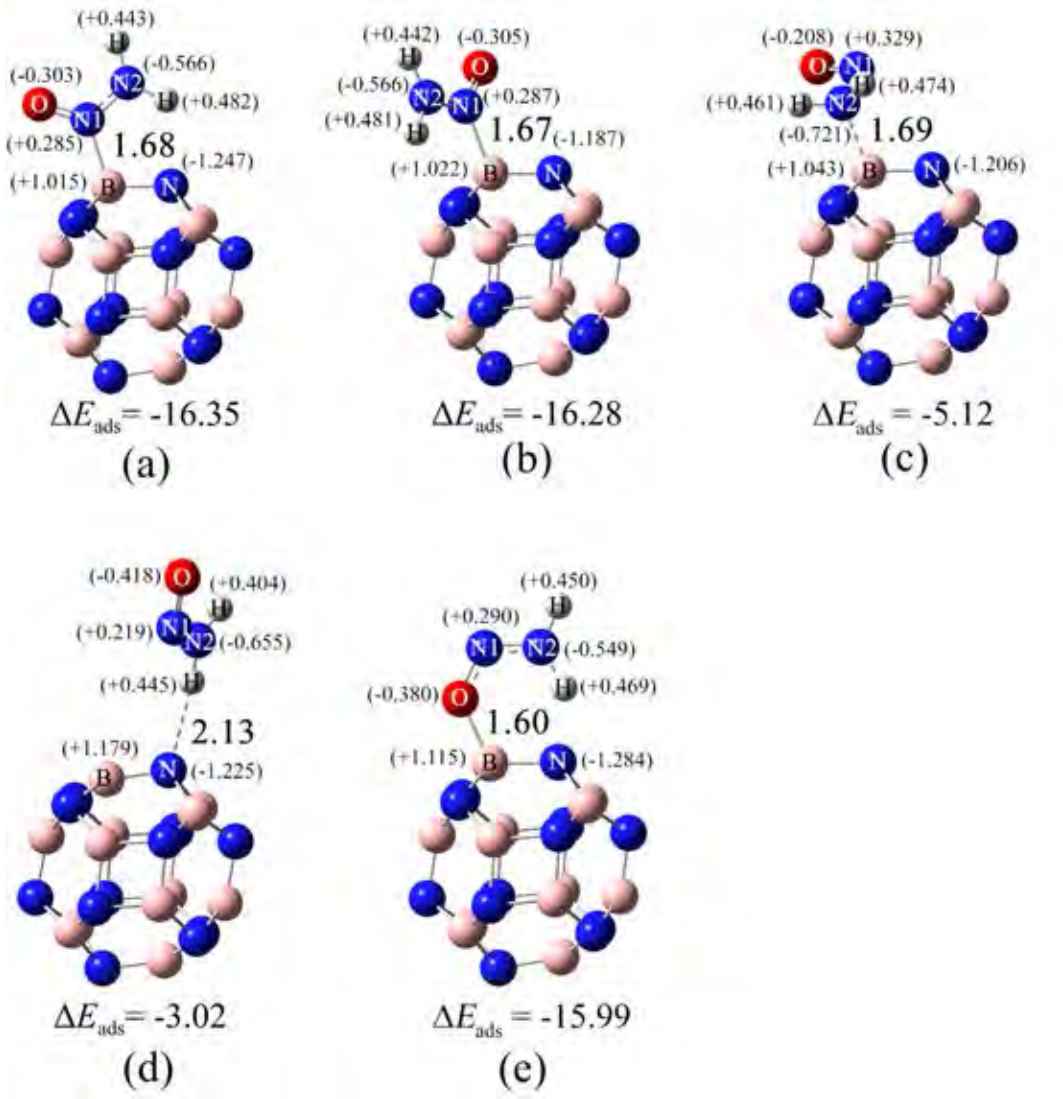

Figure 3.5 The CAM-B3LYP/6-31+G(d,p)–optimized structures of adsorption configuration of (a) *a*-nsm/BNSL-1, (b) *a*-nsm/BNSL-2, (c) *a*-nsm/BNSL-3, (d) *a*-nsm/BNSL-4 and (e) *a*-nsm/BNSL-5. Adsorption energies are in kcal/mol and bond distances are in Å.

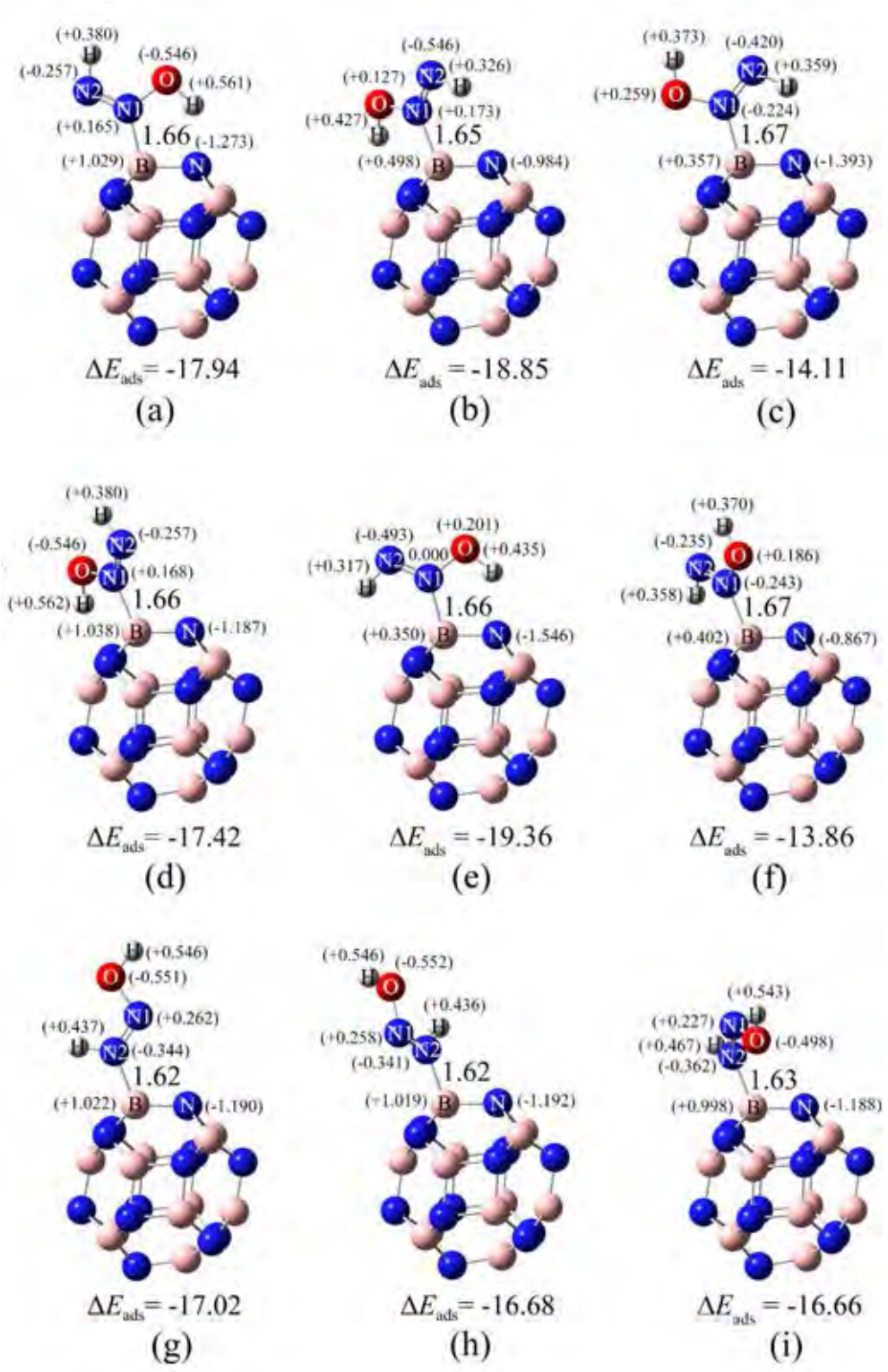

Figure 3.6 The CAM-B3LYP/6-31+G(d,p)–optimized structures of adsorption configuration of (a) *i*-nsm/BNSL-1, (b) *i*-nsm/BNSL-2, (c) *i*-nsm/BNSL-3, (d) *i*-nsm/BNSL-4, (e) *i*-nsm/BNSL-5, (f) *i*-nsm/BNSL-6, (g) *i*-nsm/BNSL-7, (h) *i*-nsm/BNSL-8 and (i) *i*-nsm/BNSL-9. Adsorption energies are in kcal/mol and bond distances are in Å.

Their stabilities are in orders: *a*–nsm/BNSL–1 > *a*–nsm/BNSL–2, > *a*–nsm/BNSL–5 > *a*–nsm/BNSL–3 > *a*–nsm/BNSL–4 for amino conformer and *i*–nsm/BNSL–5 > *i*–nsm/BNSL–2 > *i*–nsm/BNSL–1 > *i*–nsm/BNSL–4 > *i*–nsm/BNSL–7 > *i*–nsm/BNSL–8 > *i*–nsm/BNSL–9 > *i*–nsm/BNSL–3 > *i*–nsm/BNSL–6 for imino conformer. The most stable conformer of amino form, the *a*–nsm/BNSL–1 (ΔE_{ads}= –16.35 kcal/mol) is less stable than of imino form, the *i*–nsm/BNSL–5 (ΔE_{ads}= –19.36 kcal/mol) by kcal/mol by 3.01 kcal/mol. Change in electrical conductivity based on ΔE_g, it was found that sensitivities on nitrosamine adsorption of the BNSL are in the range of –14.69% to –35.85% as shown in Table 3.4.

Table 3.4 Energy gaps, adsorption energies and thermodynamic quantities of nitrosamine conformers of BNSL nanocages.

Configuration	E_g [a]	ΔE_g [b]	ΔE_{ads} [c]	ΔH^o_{ads} [d]	ΔG^o_{ads} [d]
BNSL:	9.58	–	–	–	–
a–nsm/BNSL–1	6.78	–29.22	–16.35	–16.84	–3.89
a–nsm/BNSL–2	6.85	–28.51	–16.28	–16.77	–3.79
a–nsm/BNSL–3	6.14	–35.85	–5.12	–5.34	6.56
a–nsm/BNSL–4	8.17	–14.69	–3.02	–2.42	4.87
a–nsm/BNSL–5	6.93	–27.67	–15.99	–16.55	–3.62
i–nsm/BNSL–1	7.13	–25.53	–17.94	–18.44	–5.40
i–nsm/BNSL–2	7.44	–22.31	–18.85	–19.29	–6.47
i–nsm/BNSL–3	6.88	–28.19	–14.11	–14.38	–1.80
i–nsm/BNSL–4	7.19	–24.94	–17.42	–17.90	–4.86
i–nsm/BNSL–5	7.44	–22.33	–19.36	–19.77	–7.33
i–nsm/BNSL–6	6.93	–27.62	–13.86	–14.13	–1.56
i–nsm/BNSL–7	6.48	–32.33	–17.02	–17.21	–5.16
i–nsm/BNSL–8	6.50	–32.15	–16.68	–16.84	–4.89
i–nsm/BNSL–9	6.54	–31.68	–16.66	–16.94	–4.54

[a] In eV.

[b] Percentage of energy–gap change compared with clean nanocage.

[c] Based on zero–point energy correction, in kcal/mol.

[d] At 298.15 K, in kcal/mol.

NBO atomic charges of nitrosamine conformers, atoms nearby adsorption area of the BNSL cage and PCT of bonded atoms of the cage are shown in Table 3.5.

Table 3.5 NBO atomic charges of nitrosamine conformers, atoms nearby adsorption area of the of the BNSL nanocages and partial charge transfer (PCT) of bonded atoms of nanocages.

Configuration	NBO partial charge [a]							PCT [d]	
	Nitrosamine atoms [b]					Nanocages [c]			
	O	**N1**	**N2**	**H1**	**H2**	***α***	***β***	***α***	***β***
Clean BNSL	–	–	–	–	–	1.174	–1.174	–	–
a–nsm/BNSL–1	–0.303	0.285	–0.566	0.443	0.482	1.015	–1.247	–0.159	–0.073
a–nsm/BNSL–2	–0.305	0.287	–0.566	0.481	0.442	1.022	–1.187	–0.152	–0.013
a–nsm/BNSL–3	–0.208	0.329	–0.721	0.474	0.461	1.043	–1.206	–0.131	–0.032
a–nsm/BNSL–4	–0.418	0.219	–0.655	0.445	0.404	1.179	–1.225	0.005	–0.051
a–nsm/BNSL–5	–0.380	0.290	–0.549	0.450	0.469	1.115	–1.284	–0.059	–0.110
i–nsm/BNSL–1	–0.546	0.165	–0.257	0.380	0.561	1.029	–1.273	–0.145	–0.104
i–nsm/BNSL–2	0.127	0.173	–0.546	0.326	0.427	0.498	–0.984	–0.676	0.190
i–nsm/BNSL–3	0.259	–0.224	–0.420	0.359	0.373	0.357	–1.393	–0.817	–0.219
i–nsm/BNSL–4	–0.546	0.168	–0.257	0.380	0.562	1.038	–1.187	–0.136	–0.013
i–nsm/BNSL–5	0.201	0.000	–0.493	0.317	0.435	0.350	–1.546	–0.824	–0.372
i–nsm/BNSL–6	0.186	–0.243	–0.235	0.358	0.370	0.402	–0.867	–0.772	0.307
i–nsm/BNSL–7	–0.551	0.262	–0.344	0.437	0.546	1.022	–1.190	–0.152	–0.016
i–nsm/BNSL–8	–0.552	0.258	–0.341	0.436	0.546	1.019	–1.192	–0.155	–0.018
i–nsm/BNSL–9	-0.498	0.227	-0.362	0.467	0.543	0.998	-1.188	-0.176	-0.014

[a] In e.

[b] Atoms of nitrosamine conformers defined in Fig. 3.1.

[c] Atoms of bonded atom(s) (***α*** and ***β***) of nanocages which are (***α*** = B, ***β*** = N atoms) for BNSL cages as shown in Fig. 3.1.

[d] Partial charge transfer, defined as a charge difference between adsorption–site atoms (***α*** and ***β***) of adsorption and non–adsorption states, in e.

Partial charges of binding atoms, ***α*** and ***β*** for clean BNSL cage (***α*** = 1.174 e, ***β*** = –1.174 e) and nitrosamine adsorbed cages are positive and negative, respectively, as shown in Figure 3.1. PCTs of ***α*** and ***β*** of the *a*–nsm/BNSL–4 is low which corresponds its weak interaction, see Table 3.5 and Figure 3.5(d); its adsorption energy (ΔE_{ads}= –3.02 kcal/mol) is also weak. PCTs of ***α*** and ***β*** of most adsorption configurations of *i*–nsm on the BNSL cage are negative values excepts for the *i*–nsm/BNSL–2 and *i*–nsm/BNSL–6 of which PCTs of ***β*** are positive values.

As the *i*–nsm/BNSL–1 was found to be adsorption intermediate for conversion of nitrosamine conformer to N_2 and water, the *i*–nsm/BNSL–1 is hence the starting configuration for conversion of *i*–nsm–9° isomer to water and nitrogen molecules. Energy profile of nitrosamine (*i*–nsm–9° isomer) conversion to water and nitrogen molecules on the BNSL cage as shown Figure 3.7.

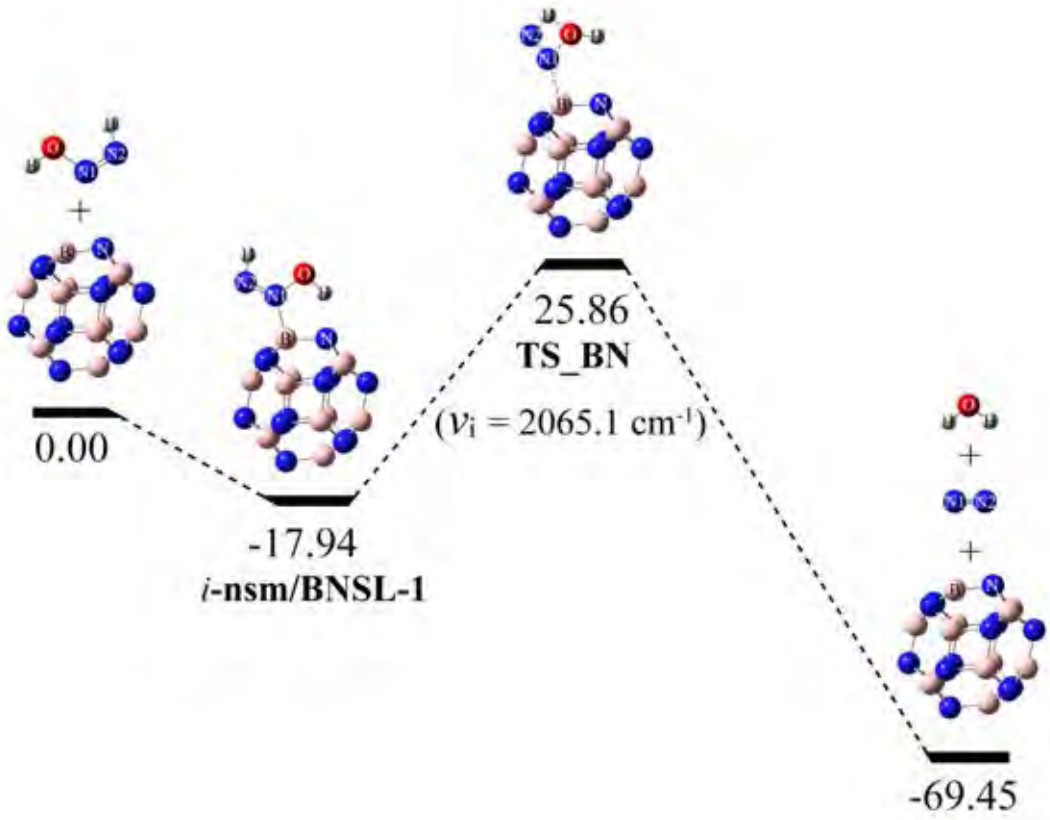

Figure 3.7 Mechanism of nitrosamine conversion to water and nitrogen on the BNSL cage. Their transition-state structures are shown at the bottom. The relative energies are in kcal/mol.

The first step is the adsorption of *i*–nsm–9° on the BNSL cage of which adsorption energy is –17.94 kcal/mol. The second step is rate determining step via transition state (TS_BN) with activation energy of 43.80 kcal/mol. The transition–state structure of TS_BN is confirmed with single–imaginary frequency of ν_i = 2065.1 cm^{-1}. The last step, nitrogen and water molecules desorb from the BNSL cage which is the energetic preferred reaction (ΔE_{react} =–51.51 kcal/mol). All two reaction steps are spontaneous processes as show in Table 3.6.

Table 3.6 Thermodynamic quantities, rate constant and equilibrium constants of reaction steps of conversion of nitrosamine to water and nitrogen molecules on the BNSL cages.

Reaction step	$\Delta^{\ddagger}E$ [a]	$\Delta^{\ddagger}G$ [b]	k_{298} [c]	ΔE [d]	ΔH^{o}_{298} [d]	ΔG^{o}_{298} [d]	K_{298}
BNSL cage:							
i–nsm+BNSL–1 → *i*–nsm/BNSL–1	–	–	–	–17.94	–18.44	–5.40	9.16×10^{3}
i–nsm/BNSL–1 → TS_BN →H_2O+N_2+BNSL	43.80	42.55	4.13×10^{-19}	–69.45	–67.69	–76.95	2.59×10^{56}

[a] Activation energy, in kcal/mol.

[b] Gibbs free energy at activation, in kcal/mol.

[c] In s^{-1}.

[d] In kcal/mol.

3.3 Adsorption and reaction on BeOSL cage

The CAM–B3LYP/6–31+G(d,p)–optimized structure of the BeOSL cage is shown in Figure 3.1. Adsorption structures of amino and imino nitrosamine conformers are shown in Figure 3.8 and Figure 3.9, respectively. All adsorption structures of amino and imino nitrosamine conformers are five and nine configurations respectively.

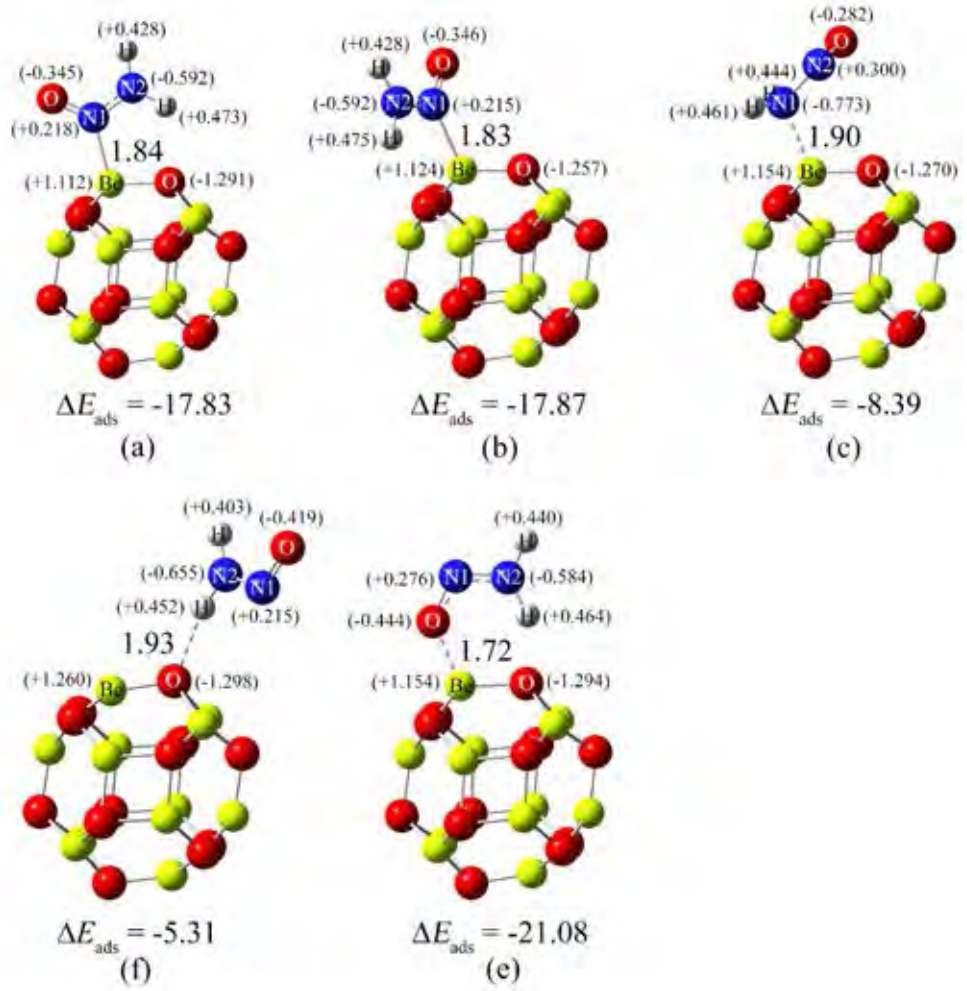

Figure 3.8 The CAM-B3LYP/6-31+G(d,p)–optimized structures of adsorption configuration of (a) *a*-nsm/BeOSL-1, (b) *a*-nsm/BeOSL-2, (c) *a*-nsm/BeOSL-3, (d) *a*-nsm/BeOSL-4 and (e) *a*-nsm/BeOSL-5. Adsorption energies are in kcal/mol and bond distances are in Å.

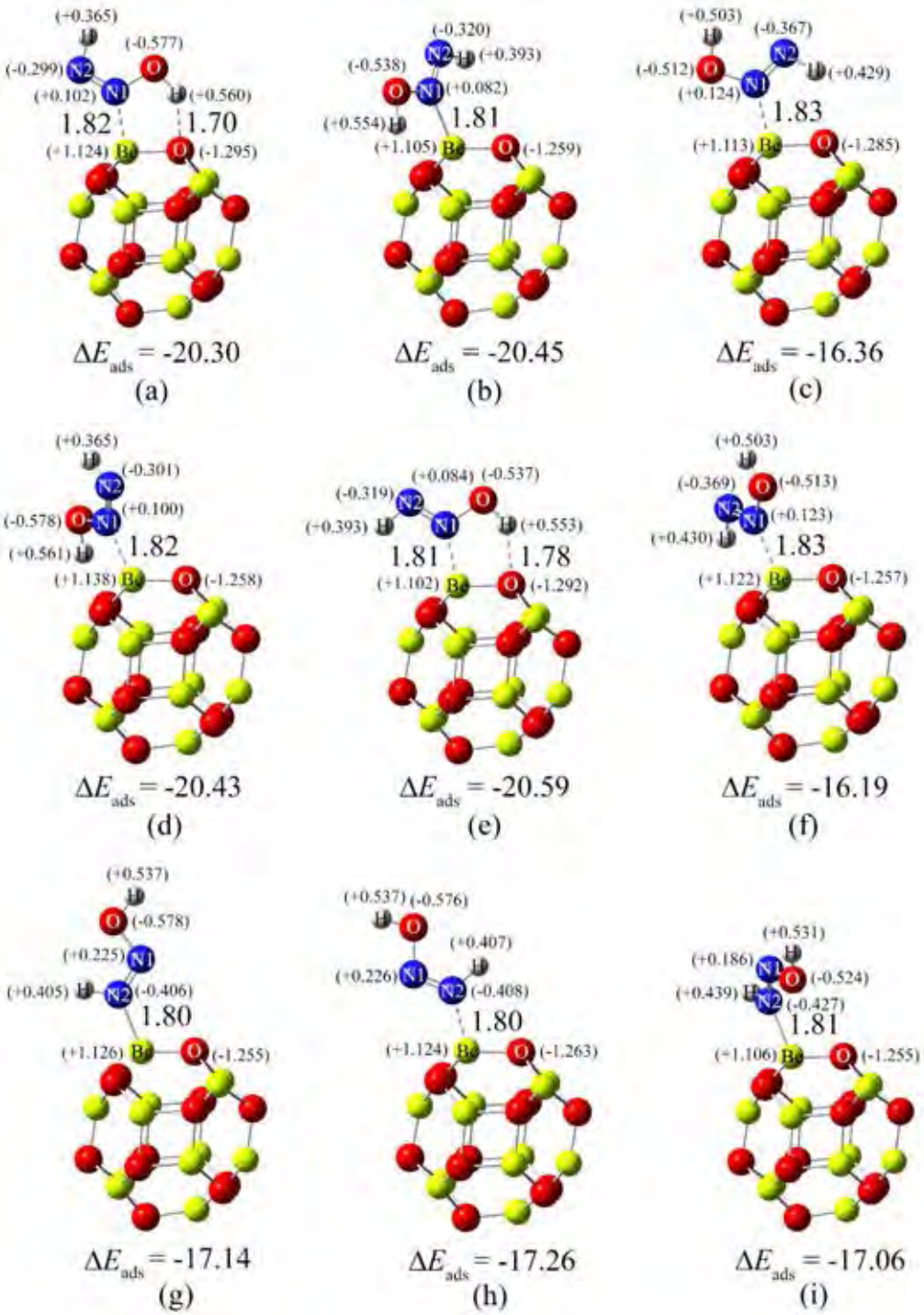

Figure 3.9 The CAM-B3LYP/6-31+G(d,p)–optimized structures of adsorption configuration of (a) *i*-nsm/BeOSL-1, (b) *i*-nsm/BeOSL-2, (c) *i*-nsm/BeOSL-3, (d) *i*-nsm/BeOSL-4, (e) *i*-nsm/BeOSL-5, (f) *i*-nsm/BeOSL-6, (g) *i*-nsm/BeOSL-7, (h) *i*-nsm/BeOSL-8 and (i) *i*-nsm/BeOSL-9. Adsorption energies are in kcal/mol and bond distances are in Å.

Their stabilities are in orders: *a*–nsm/BeOSL–5 > *a*–nsm/BeOSL–2 > *a*–nsm/BeOSL–1 > *a*–nsm/BeOSL–3 > *a*–nsm/BeOSL–4 for amino conformer and *i*–nsm/BeOSL–5 > *i*–nsm/BeOSL–2 > *i*–nsm/BeOSL–4 > *i*–nsm/BeOSL–1 > *i*–nsm/BeOSL–8 > *i*–nsm/BeOSL–7 > *i*–nsm/BeOSL–9 > *i*–nsm/BeOSL–3 > *i*–nsm/BeOSL–6 for imino conformer. Adsorptions for all *i*–nsm/BeOSL configurations are strong and their adsorption energies are within the ranges of –20.59 to –16.19 kcal/mol. The most stable conformer of amino form, the *a*–nsm/ BeOSL–5 (ΔE_{ads}= –21.08 kcal/mol) is more stable than of imino form, the *i*–nsm/BeOSL–5 (ΔE_{ads}= –20.59 kcal/mol) by kcal/mol by 0.49 kcal/mol.

According to change in electrical conductivity based on ΔE_g, sensitivities on nitrosamine adsorption of the BeOSL in the range within –8.31% to –21.18%, were found that as shown in Table 3.7.

Table 3.7 Energy gaps, adsorption energies and thermodynamic quantities of nitrosamine conformers of BeOSL nanocages.

Configuration	E_g [a]	ΔE_g [b]	ΔE_{ads} [c]	ΔH^o_{ads} [d]	ΔG^o_{ads} [d]
BeOSL:	10.15	–	–	–	–
a–nsm/BeOSL–1	8.59	–15.35	–17.83	–18.04	–5.93
a–nsm/BeOSL–2	8.58	–15.43	–17.87	–18.07	–5.94
a–nsm/BeOSL–3	8.08	–20.44	–8.39	–8.35	2.46
a–nsm/BeOSL–4	8.00	–21.18	–5.31	–5.45	5.40
a–nsm/BeOSL–5	8.67	–14.58	–21.08	–21.39	–9.02
i–nsm/BeOSL–1	9.00	–11.32	–20.30	–20.53	–8.28
i–nsm/BeOSL–2	9.31	–8.31	–20.45	–20.63	–8.56
i–nsm/BeOSL–3	8.72	–14.11	–16.36	–16.35	–4.71
i–nsm/BeOSL–4	9.09	–10.48	–20.43	–20.65	–8.37
i–nsm/BeOSL–5	9.29	–8.48	–20.59	–20.77	–8.82
i–nsm/BeOSL–6	8.78	–13.53	–16.19	–16.18	–4.49
i–nsm/BeOSL–7	8.34	–17.87	–17.14	–16.96	–6.49
i–nsm/BeOSL–8	8.23	–18.95	–17.26	–17.10	–6.33
i–nsm/BeOSL–9	8.40	–17.20	–17.06	–16.97	–5.94

[a] In eV.

[b] Percentage of energy–gap change compared with clean nanocage.

[c] Based on zero–point energy correction, in kcal/mol.

[d] At 298.15 K, in kcal/mol.

NBO atomic charges of nitrosamine conformers, atoms nearby adsorption area of the BeOSL cage and PCT of bonded atoms of the cage are shown in Table 3.8. Partial charges of binding atoms, ***α*** and ***β*** for clean BeOSL cage (***α*** = 1.259 e, ***β*** = –1.259 e) and nitrosamine adsorbed cages are positive and negative, respectively, as shown in Figures 3.8 and 3.9. Only the PCT of ***α*** of *a*–nsm/BeOSL–4 is lowest value which corresponds its weak interaction, see Table 3.7 and Figure 3.8(f); its adsorption energy (ΔE_{ads}= –5.31 kcal/mol) is somewhat weak. As all PCTs of ***β*** of most adsorption configurations of *i*–nsm on the BeOSL cage are low (both positive and negative), their ***β*** atoms were found to be low effect on adsorptions.

Table 3.8 NBO atomic charges of nitrosamine conformers, atoms nearby adsorption area of the BeOSL nanocages and partial charge transfer (PCT) of bonded atoms of nanocages.

Configuration	NBO partial charge [a]							PCT [d]	
	Nitrosamine atoms [b]					Nanocages [c]			
	O	**N1**	**N2**	**H1**	**H2**	***α***	***β***	***α***	***β***
Clean BeOSL	–	–	–	–	–	1.259	–1.259	–	–
a–nsm/BeOSL–1	–0.345	0.218	–0.592	0.428	0.473	1.112	–1.291	–0.147	–0.032
a–nsm/BeOSL–2	–0.346	0.215	–0.592	0.475	0.428	1.124	–1.257	–0.135	0.002
a–nsm/BeOSL–3	–0.282	0.300	–0.773	0.444	0.461	1.154	–1.270	–0.105	–0.011
a–nsm/BeOSL–4	–0.419	0.215	–0.655	0.403	0.452	1.260	–1.298	0.001	–0.039
a–nsm/BeOSL–5	–0.444	0.276	–0.584	0.440	0.464	1.154	–1.294	–0.105	–0.035
i–nsm/BeOSL–1	–0.577	0.102	–0.299	0.560	0.365	1.124	–1.295	–0.135	–0.036
i–nsm/BeOSL–2	–0.538	0.082	–0.320	0.393	0.554	1.105	–1.259	–0.154	0.000
i–nsm/BeOSL–3	–0.512	0.124	–0.367	0.503	0.429	1.113	–1.285	–0.146	–0.026
i–nsm/BeOSL–4	–0.578	0.100	–0.301	0.561	0.365	1.138	–1.258	–0.121	0.001
i–nsm/BeOSL–5	–0.537	0.084	–0.319	0.393	0.553	1.102	–1.292	–0.157	–0.033
i–nsm/BeOSL–6	–0.513	0.123	–0.369	0.503	0.430	1.122	–1.257	–0.137	0.002
i–nsm/BeOSL–7	–0.578	0.225	–0.406	0.537	0.405	1.126	–1.255	–0.133	0.004
i–nsm/BeOSL–8	–0.576	0.226	–0.408	0.407	0.537	1.124	–1.263	–0.135	–0.004
i–nsm/BeOSL–9	–0.524	0.186	–0.427	0.439	0.531	1.106	–1.255	–0.153	0.004

[a] In e.

[b] Atoms of nitrosamine conformers defined in Figure 3.1.

[c] Atoms of bonded atom(s) (***α*** and ***β***) of nanocages which are (***α*** = Be, ***β*** = O atoms) for BeOSL cages as shown in Figure 3.1.

[d] Partial charge transfer, defined as a charge difference between adsorption–site atoms (***α*** and ***β***) of adsorption and non–adsorption states, in e.

As the *i*–nsm/BeOSL–1 was found to be adsorption intermediate for conversion of nitrosamine conformer to N_2 and water, the *i*–nsm/BeOSL–1 is used as the starting configuration for conversion of *i*–nsm–9° isomer to water and nitrogen molecules. Energy profile of nitrosamine (*i*–nsm–9° isomer) conversion to water and nitrogen molecules on the BeOSL cage as shown Figure 3.10. The first step is the adsorption of *i*–nsm–9° on the BeOSL cag of which adsorption energy is –20.30 kcal/mol. The second step is rate determining step via transition state (TS_BeO) with activation energy of 39.17 kcal/mol. The transition–state structure of TS_BeO is confirmed with single–imaginary frequency of ν_i = 1970.3 cm^{-1}. The last step, nitrogen and water molecules desorb from the BeOSL cage which is the energetic preferred reaction (ΔE_{react} =–49.15 kcal/mol). All two reaction steps are spontaneous processes as show in Table 3.9.

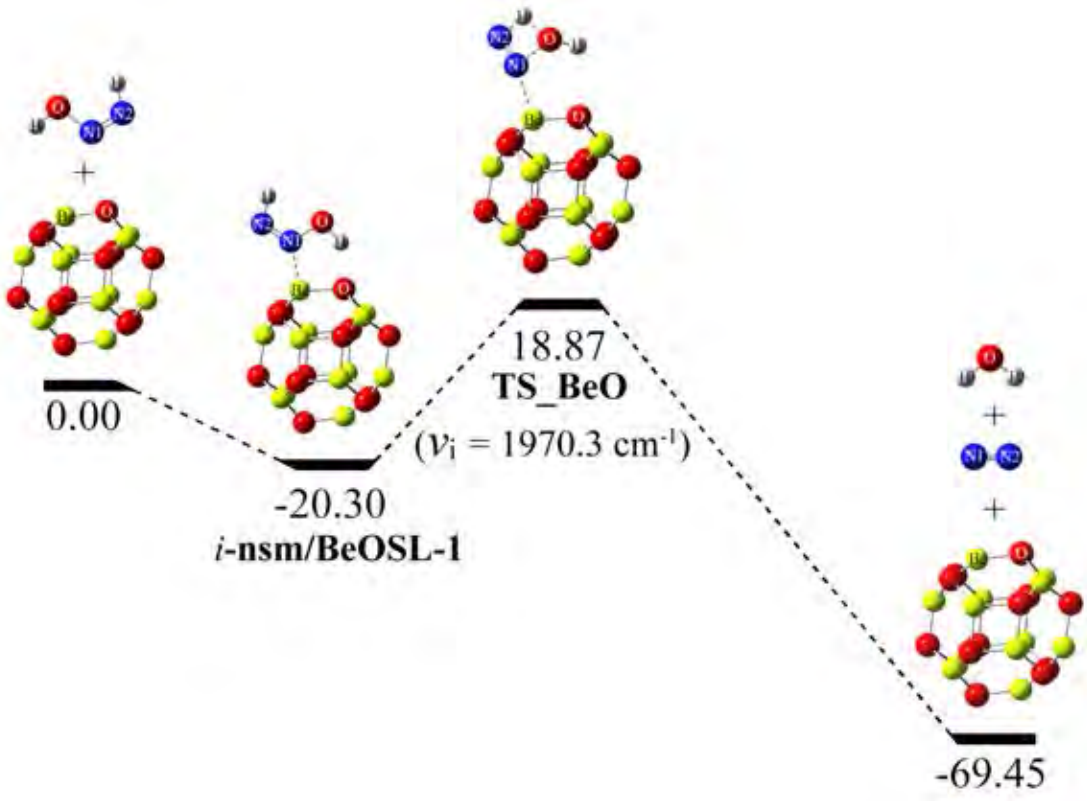

Figure 3.10 Mechanism of nitrosamine (*i*-nsm/BeOSL-1) conversion to water and nitrogen on the BeOSL cage. Their transition-state structures are shown at the bottom. The relative energies are in kcal/mol.

Table 3.9 Thermodynamic quantities, rate constant and equilibrium constants of reaction steps of conversion of nitrosamine to water and nitrogen molecules on the BeOSL cages.

Reaction step	$\Delta^{\ddagger}E$ [a]	$\Delta^{\ddagger}G$ [b]	k_{298} [c]	ΔE [d]	ΔH^{o}_{298} [d]	ΔG^{o}_{298} [d]	K_{298}
BeOSL cage:							
i–nsm+BeOSL–1 → *i*–nsm/BeOSL–1	–	–	–	–20.30	–20.53	–8.28	1.17×10^{6}
i–nsm/BeOSL–1→ **TS_BeO** → H_2O+N_2+BeOSL	39.17	37.87	1.12×10^{-15}	–69.45	–67.69	–76.95	2.59×10^{56}

[a] Activation energy, in kcal/mol.

[b] Gibbs free energy at activation, in kcal/mol.

[c] In s^{-1}.

[d] In kcal/mol.

3.4 Adsorption and reaction on AlPSL cage

The CAM–B3LYP/6–31+G(d,p)–optimized structure of the AlPSL cage is shown in Figure 3.1. Adsorption structures of amino and imino nitrosamine conformers are shown in Figure 3.11 and Figure 3.12, respectively. All adsorption structures of amino and imino nitrosamine conformers are four and ten configurations respectively. Their stabilities are in orders: *a*–nsm/AlPSL–4 > *a*–nsm/AlPSL–2 > *a*–nsm/AlPSL–1 > *a*–nsm/AlPSL–3 for amino conformer and *i*–nsm/AlPSL–10 > *i*–nsm/AlPSL–7 > *i*–nsm/AlPSL–9 > *i*–nsm/AlPSL–8 > *i*–nsm/AlPSL–5 > *i*–nsm/AlPSL–2 > *i*–nsm/AlPSL–4 > *i*–nsm/AlPSL–1 > *i*–nsm/AlPSL–6 > *i*–nsm/AlPSL–3 for imino conformer. Adsorption energies for all *a*–nsm/AlPSL configurations as shown in Table 3.10 are within the ranges of –19.23 to –7.47 kcal/mol and for all *i*–nsm/AlPSL configurations as also shown in Table 3.10 are within the ranges of –19.28 to –15.02 kcal/mol. The most stable conformer of amino form, the *a*–nsm/ AlPSL–4 (ΔE_{ads}= –19.23 kcal/mol) and imino form, the *i*–nsm/AlPSL–5 (ΔE_{ads}= –19.28 kcal/mol) are hardly different. Change in electrical conductivity based on ΔE_g, sensitivities on nitrosamine adsorption of the AlPSL in the range of –0.15% to –6.74%, were obtained.

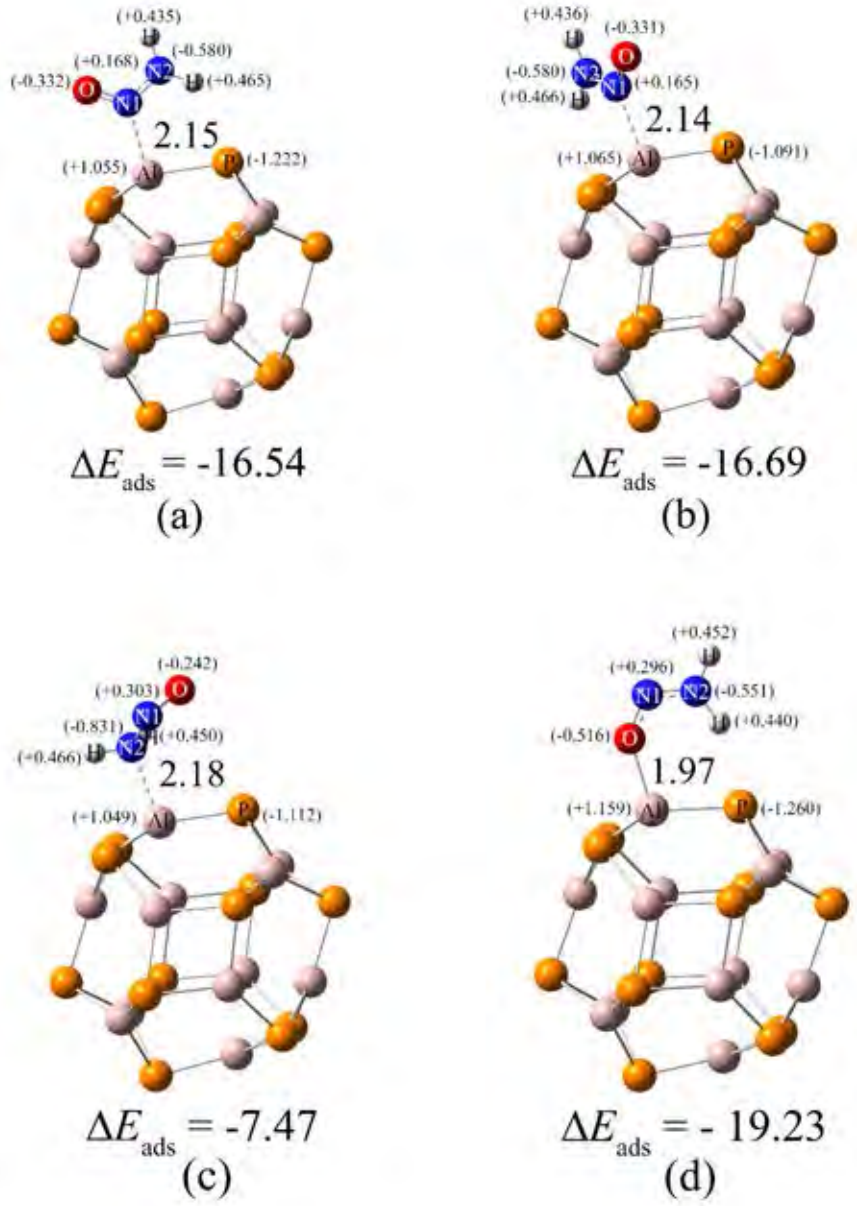

Figure 3.11 The CAM-B3LYP/6-31+G(d,p)–optimized structures of adsorption configuration of (a) *a*-nsm/AlPSL-1, (b) *a*-nsm/AlPSL-2, (c) *a*-nsm/AlPSL-3, (d) *a*-nsm/AlPSL-4 and (e) *a*-nsm/AlPSL-5. Adsorption energies are in kcal/mol and bond distances are in Å.

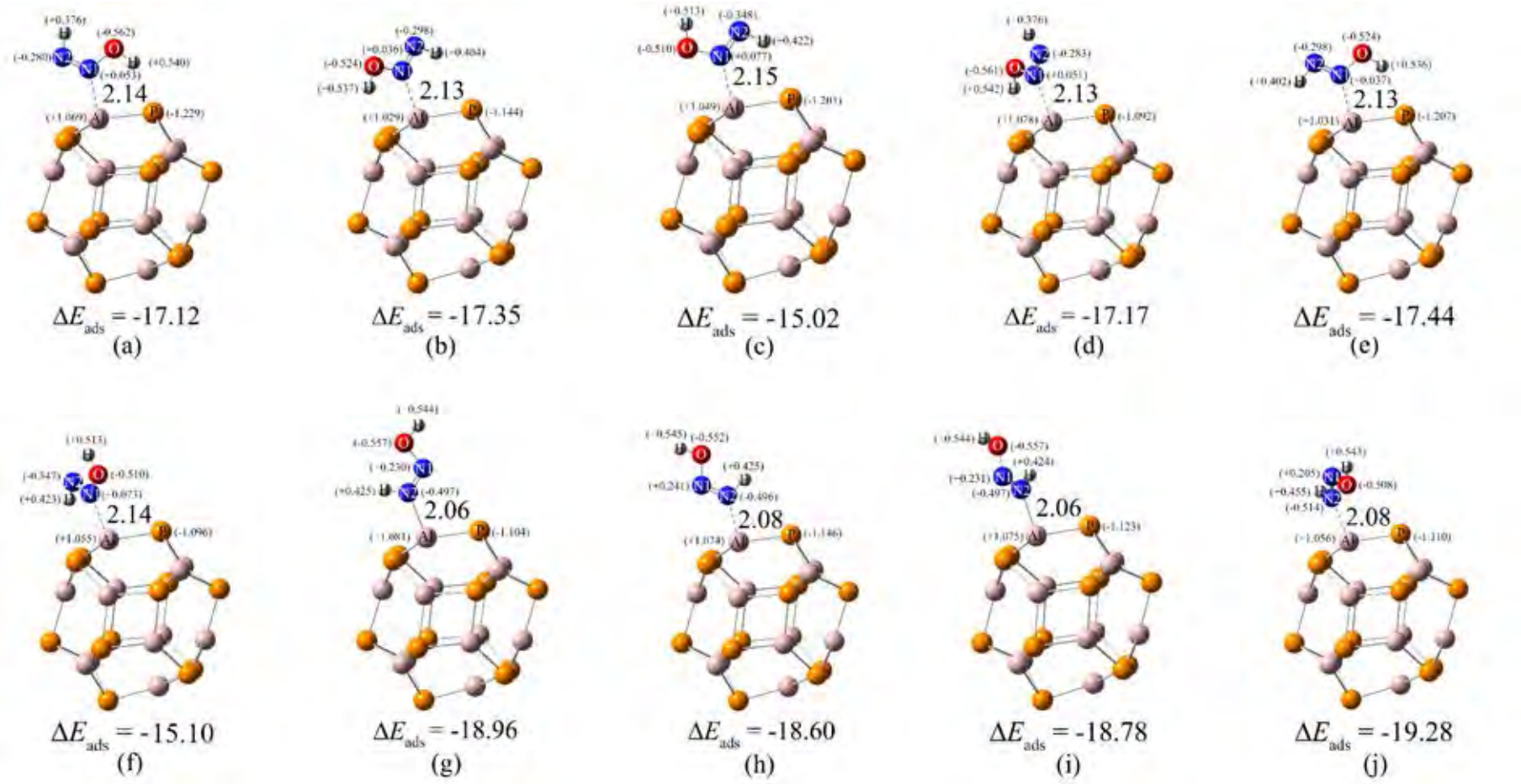

Figure 3.12 The CAM-B3LYP/6-31+G(d,p)–optimized structures of adsorption configuration of (a) *i*-nsm/AlPSL-1, (b) *i*-nsm/AlPSL-2, (c) *i*-nsm/AlPSL-3, (d) *i*-nsm/AlPSL-4, (e) *i*-nsm/AlPSL-5, (f) *i*-nsm/AlPSL-6, (g) *i*-nsm/AlPSL-7, (h) *i*-nsm/AlPSL-8, (i) *i*-nsm/AlPSL-9 and (j) *i*-nsm/AlPSL-10. Adsorption energies are in kcal/mol and bond distances are in Å.

Table 3.10 Energy gaps, adsorption energies and thermodynamic quantities of nitrosamine conformers of AlPSL nanocages.

Configuration	E_g [a]	ΔE_g [b]	ΔE_{ads} [c]	ΔH^o_{ads} [d]	ΔG^o_{ads} [d]
AlPSL:	5.70	–	–	–	–
a–nsm/AlPSL–1	5.62	–1.30	–16.54	–16.69	–4.77
a–nsm/AlPSL–2	5.64	–1.07	–16.69	–16.85	–4.87
a–nsm/AlPSL–3	5.37	–5.68	–7.47	–7.42	3.52
a–nsm/AlPSL–4	5.54	–2.69	–19.23	–19.43	–7.63
i–nsm/AlPSL–1	5.63	–1.23	–17.12	–17.24	–5.31
i–nsm/AlPSL–2	5.69	–0.15	–17.35	–17.47	–5.55
i–nsm/AlPSL–3	5.64	–0.95	–15.02	–14.96	–3.44
i–nsm/AlPSL–4	5.64	–1.01	–17.17	–17.30	–5.30
i–nsm/AlPSL–5	5.67	–0.38	–17.44	–17.53	–5.88
i–nsm/AlPSL–6	5.65	–0.81	–15.10	–15.06	–3.46
i–nsm/AlPSL–7	5.46	–4.17	–18.96	–18.84	–7.91
i–nsm/AlPSL–8	5.31	–6.74	–18.60	–18.98	–6.54
i–nsm/AlPSL–9	5.47	–4.06	–18.78	–18.64	–7.77
i–nsm/AlPSL–10	5.43	–4.74	–19.28	–19.23	–7.88

[a] In eV.

[b] Percentage of energy–gap change compared with clean nanocage.

[c] Based on zero–point energy correction, in kcal/mol.

[d] At 298.15 K, in kcal/mol.

NBO atomic charges of nitrosamine conformers, atoms nearby adsorption area of the AlPSL cage and PCT of bonded atoms of the cage are shown in Table 3.11.

Table 3.11 NBO atomic charges of nitrosamine conformers, atoms nearby adsorption area of the AlPSL nanocages and partial charge transfer (PCT) of bonded atoms of nanocages.

Configuration	NBO partial charge [a]							PCT [d]	
	Nitrosamine atoms [b]					Nanocages [c]			
	O	**N1**	**N2**	**H1**	**H2**	***α***	***β***	***α***	***β***
Clean AlPSL	–	–	–	–	–	1.060	–1.060	–	–
a–nsm/AlPSL–1	–0.332	0.168	–0.580	0.465	0.435	1.055	–1.222	–0.005	–0.162
a–nsm/AlPSL–2	–0.331	0.165	–0.580	0.466	0.436	1.065	–1.091	0.005	–0.031
a–nsm/AlPSL–3	–0.242	0.303	–0.831	0.450	0.466	1.049	–1.112	–0.011	–0.052
a–nsm/AlPSL–4	–0.516	0.296	–0.551	0.452	0.440	1.159	–1.260	0.099	–0.200
i–nsm/AlPSL–1	–0.562	0.053	–0.280	0.540	0.376	1.069	–1.229	0.009	–0.169
i–nsm/AlPSL–2	–0.524	0.036	–0.298	0.404	0.537	1.029	–1.144	–0.031	–0.084
i–nsm/AlPSL–3	–0.510	0.077	–0.348	0.513	0.422	1.049	–1.201	–0.011	–0.141
i–nsm/AlPSL–4	–0.561	0.051	–0.283	0.376	0.542	1.078	–1.092	0.018	–0.032
i–nsm/AlPSL–5	–0.524	0.037	–0.298	0.536	0.402	1.031	–1.207	–0.029	–0.147
i–nsm/AlPSL–6	–0.510	0.073	–0.347	0.513	0.423	1.055	–1.096	–0.005	–0.036
i–nsm/AlPSL–7	–0.557	0.230	–0.497	0.544	0.425	1.081	–1.104	0.021	–0.044
i–nsm/AlPSL–8	–0.552	0.241	–0.496	0.545	0.425	1.074	–1.146	0.014	–0.086
i–nsm/AlPSL–9	–0.557	0.231	–0.497	0.424	0.544	1.075	–1.123	0.015	–0.063
i–nsm/AlPSL–10	–0.508	0.205	–0.514	0.455	0.543	1.056	–1.110	–0.004	–0.050

[a] In e.

[b] Atoms of nitrosamine conformers defined in Fig. 3.1.

[c] Atoms of bonded atom(s) (***α*** and ***β***) of nanocages which are (***α*** = Al, ***β*** = P atoms) for AlPSL cages, respectively as shown in Fig. 3.1.

[d] Partial charge transfer, defined as a charge difference between adsorption–site atoms (***α*** and ***β***) of adsorption and non–adsorption states, in e.

Partial charges of binding atoms, ***α*** and ***β*** for clean AlPSL cage (***α*** = 1.060 e, ***β*** = –1.060 e) and nitrosamine adsorbed cages are positive and negative, respectively, as shown in Figures. 3.11 and 3.12. Only the PCT of ***α*** of *a*–nsm/AlPSL–3 is lowest value which corresponds its weak interaction, see Table 3.11 and Figure 3.11(c); its adsorption energy (ΔE_{ads}= –7.47 kcal/mol) is rather weak. As all PCTs of ***β*** of most adsorption configurations of *i*–nsm on the AlPSL cage are low (both positive and negative), their ***β*** atoms were found to be low effect on adsorptions.

As the *i*–nsm/AlPSL–1 was found to be adsorption intermediate for conversion of nitrosamine conformer to N_2 and water, the *i*–nsm/AlPSL–1 is used as the starting configuration for conversion of *i*–nsm–9° isomer to water and nitrogen molecules. Energy profile of nitrosamine

(i–nsm–9° isomer) conversion to water and nitrogen molecules on the AlPSL cage as shown Figure 3.13. The first step is the adsorption of i–nsm–9° on the AlPSL cage of which adsorption energy is –17.12 kcal/mol. The second step is rate determining step via transition state (TS_BeO) with activation energy of 37.02 kcal/mol. The transition–state structure of TS_BeO is confirmed with single–imaginary frequency of ν_i = 1916.7 cm^{-1}. The last step, nitrogen and water molecules desorb from the AlPSL cage which is the energetic preferred reaction (ΔE_{react} =–52.33 kcal/mol). All two reaction steps are spontaneous processes as show in Table 3.5.

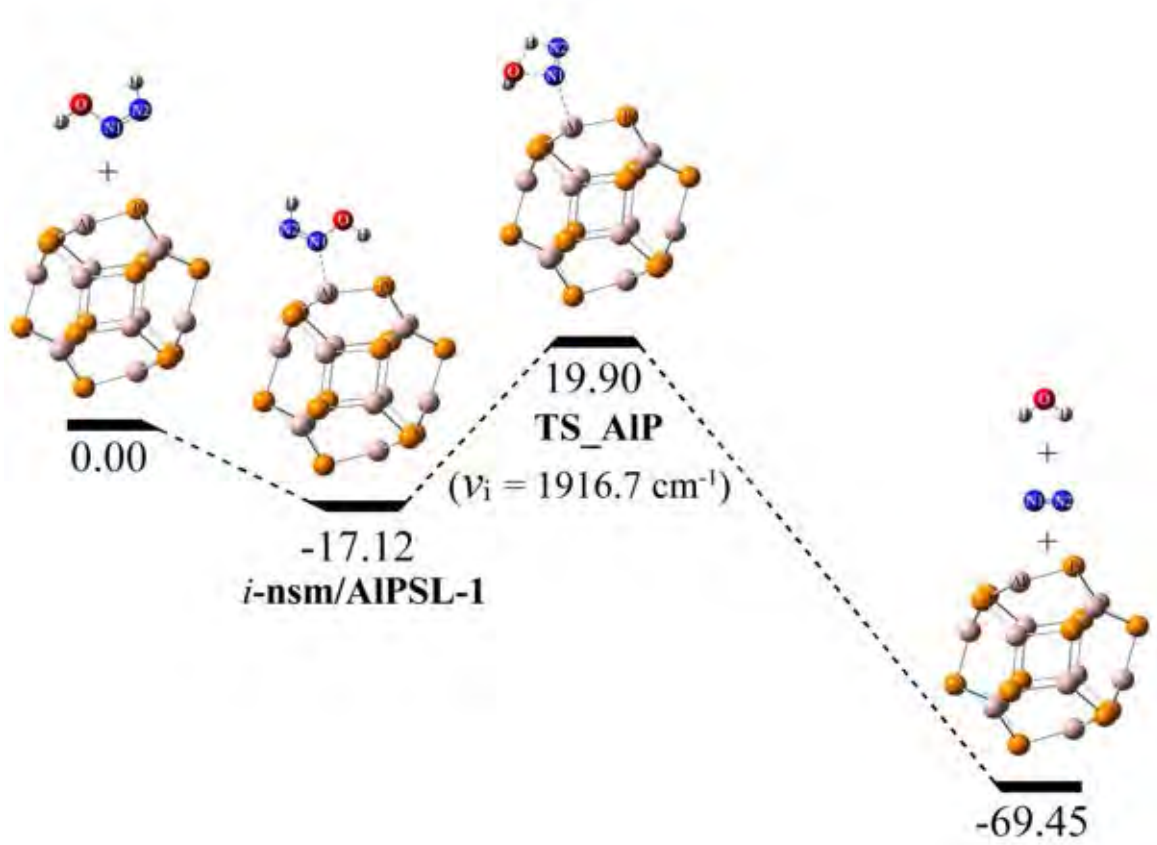

Figure 3.13 Mechanism of nitrosamine conversion to water and nitrogen on the AlPSL cage. Their transition-state structures are shown at the bottom. The relative energies are in kcal/mol.

Table 3.12 Thermodynamic quantities, rate constant and equilibrium constants of reaction steps of conversion of nitrosamine to water and nitrogen molecules on the AlPSL cages.

Reaction step	$\Delta^{\ddagger}E$ [a]	$\Delta^{\ddagger}G$ [b]	k_{298} [c]	ΔE [d]	ΔH^{o}_{298} [d]	ΔG^{o}_{298} [d]	K_{298}
AlPSL cage:							
i–nsm+AlPSL–1 → *i*–nsm/AlPSL–1	–	–	–	–17.12	–17.24	–5.31	7.82×10^{3}
i–nsm/AlPSL–1→ **TS_AlP** → H_2O+N_2+AlPSL	37.02	36.03	2.42×10^{-14}	–69.45	–67.69	–76.95	2.59×10^{56}

[a] Activation energy, in kcal/mol.

[b] Gibbs free energy at activation, in kcal/mol.

[c] In s^{-1}.

[d] In kcal/mol.

3.5 Comparison of reaction on all the nanocages

The adsorption abilities of all the nanocages on nitrosamine adsorption are in order: *a*–nsm–1/CSL (ΔE_{ads}= –37.63 kcal/mol) >> *a*–nsm–5/BeOSL (ΔE_{ads}= –21.08 kcal/mol) > *a*–nsm–4/AlPSL (ΔE_{ads}= –19.23 kcal/mol) > *a*–nsm–1/BNSL (ΔE_{ads}= –16.35 kcal/mol) for amino conformation and *i*–nsm–1/CSL (ΔE_{ads}= –26.22 kcal/mol) >> *i*–nsm–5/BeOSL (ΔE_{ads}= –20.59 kcal/mol) > *i*–nsm–5/BNSL (ΔE_{ads}= –19.36 kcal/mol) > *i*–nsm–10/AlPSL (ΔE_{ads}= –19.28 kcal/mol) for imino conformation, respectively. As electrical conductivity based on ΔE_g (in percent), sensitivities on nitrosamine adsorption of nano–cages are in order: BNSL (within the range of –14.69% to –35.85%) > BeOSL (–8.31% to –21.18%) > AlPSL (–0.15% to –6.74%) > CSL (–0.09% to –3.29%). All reaction steps for conversion nitrosamine to water and nitrogen molecules either on CSL or BNSL or BeOSL or AlPSL nano–cage are exothermic and spontaneous reactions. Due to a comparison of activation energies of nitrosamine conversion to water and nitrogen molecule on all studied nanocages is shown in Figure 3.14, it was found that reaction abilities are in order: AlPSL > BeOSL >> BNSL > CSL.

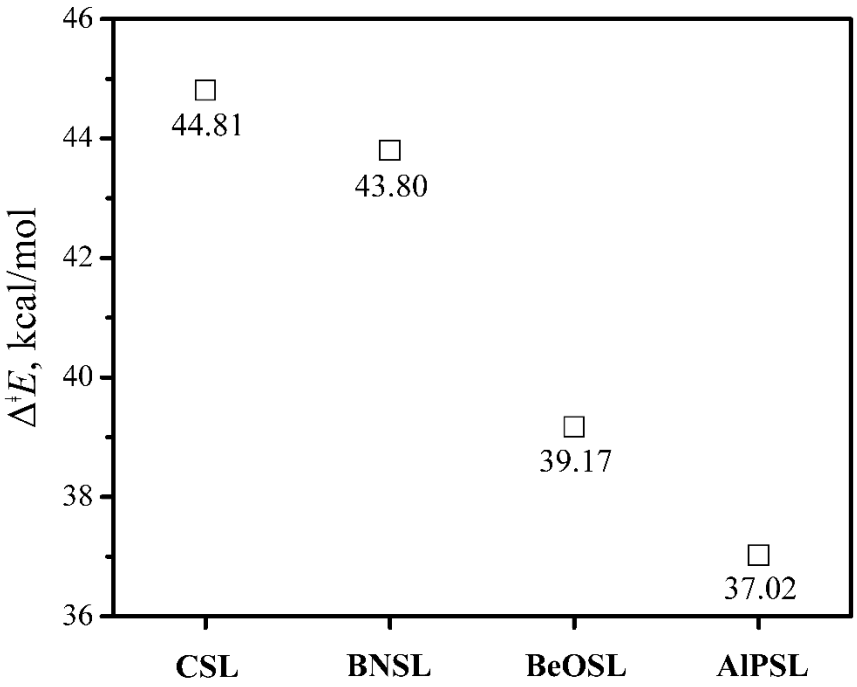

Figure 3.14 Plot of activation energy of nitrosamine conversion to nitrogen gas and water on various sodalite-like nanocages.

CHAPTER IV

CONCLUSIONS

The adsorption structure of nitrosamine conformers on four type nano-cages; CSL, BNSL, BeOSL and AlPSL for all possible configurations were calculated using CAM-B3LYP/6-31+G(d,p) method. From the result of calculations can be concluded as follow:

- The adsorption abilities of nano–cages on nitrosamine are in order: CSL >> BeOSL > AlPSL > BNSL for amino conformation and CSL >> BeOSL > BNSL > AlPSL for imino conformation, respectively that based on most stable configurations.
- The sensitivities on nitrosamine adsorption of nano–cages are in order: BNSL > BeOSL > AlPSL > CSL.
- All reaction steps for conversion nitrosamine to water and nitrogen molecules either on CSL or BNSL or BeOSL or AlPSL nano-cage are exothermic and spontaneous reactions.
- Reaction abilities to conversion nitrosamine to water and nitrogen molecules are in order: AlPSL > BeOSL >> BNSL > CSL.

The four type sodalite-like cages; CSL, BNSL, BeOSL and AlPSL can be used to storage gas and catalyze in conversion reaction that convert the toxic gas such as nitrosamine to non-toxic gas (water and nitrogen). The overall reaction is exothermic process and spontaneous reaction as suggest by Gibbs free energy at 298 K.

REFERENCES

[1] IARC, Some N-nitroso compounds, IARC Monographs on the Evaluation of the Carcinogenic Risk of Chemicals to Humans, IARC, Lyon, 1978.

[2] H. Biaudet, T. Mavelle, G. Debry, Mean daily intake of N-nitrosodimethylamine from foods and beverages in France in 1987-1992, Food and Chemical Toxicology, 32 (1994) 417-421.

[3] N.P. Sen, S. Seaman, An Investigation into the Possible Presence of Volatile N-Nitrosamines in Cooking Oils, Margarine, and Butter, Journal of Agricultural and Food Chemistry, 29 (1981) 787-789.

[4] S. Yurchenko, U. Mölder, N-nitrosodimethylamine analysis in Estonian beer using positive-ion chemical ionization with gas chromatography mass spectrometry, Food Chemistry, 89 (2005) 455-463.

[5] N.P. Sen, Formation and occurrence of nitrosamines in food, Diet, Nutrition and Cancer: A Critical Evaluation: Volume II: Micronutrients, Nonnutritive Dietary Factors, and Cancer2018, pp. 135-160.

[6] X. Zheng, T. Xu, R. Shi, N. Lu, J. Zhang, C. Jiang, C. Zhang, J. Zhou, Preparation of hollow porous molecularly imprinted polymers for N-nitrosamine adsorption, Materials Letters, 211 (2018) 21-23.

[7] Z.Y. Yun, Y. Xu, J.H. Xu, Z.Y. Wu, Y.I. Wei, Z.P. Zhou, J.H. Zhu, In situ FTIR investigation on the adsorption of nitrosamines in zeolites, Microporous and Mesoporous Materials, 72 (2004) 127-135.

[8] A. Pinisakul, C. Kritayakornupong, V. Ruangpornvisuti, Molecular modeling of nitrosamines adsorbed on H-ZSM-5 zeolite: An ONIOM study, Journal of Molecular Modeling, 14 (2008) 1035-1041.

[9] H. Roohi, M. Jahantab, Adsorption of parent nitrosamine on the nanocrystaline M-ZSM-5 zeolite: A density functional study, Journal of Chemical Sciences, 125 (2013) 1607-1618.

[10] H. Roohi, M. Jahantab, Adsorption sensitivity of nanocrystalline B-substituted H-ZSM-5 and alkali metal-exchanged M-ZSM-5 zeolites towards parent nitrosamine: A B97D study, Computational and Theoretical Chemistry, 1066 (2015) 76-87.

[11] V. Ruangpornvisuti, Molecular modeling of dissociative and non-dissociative chemisorption of nitrosamine on close-ended and open-ended pristine and Stone-Wales defective (5,5) armchair single-walled carbon nanotubes, Journal of Molecular Modeling, 16 (2010) 1127-1138.

[12] B. Shen, L.L. Ma, J.H. Zhu, Q.H. Xu, Decomposition of N-nitrosamines over zeolites, Chemistry Letters, (2000) 380-381.

[13] M.T. Baei, M. Moghimi, A. Shojaei, Benzene adsorption on C<inf>24</inf> Fullerene, Biosciences Biotechnology Research Asia, 12 (2015) 1363-1366.

[14] Y. Zhang, X. Cheng, Hydrogen storage property of alkali and alkaline-earth metal atoms decorated C24 fullerene: A DFT study, Chemical Physics, 505 (2018) 26-33.

[15] A. Hosseinian, E. Vessally, S. Yahyaei, L. Edjlali, A. Bekhradnia, A Density Functional Theory Study on the Interaction Between 5-Fluorouracil Drug and C_{24} Fullerene, Journal of Cluster Science, 28 (2017) 2681-2692.

[16] A. Gholami, A.R. Ashrafi, Calculation of the symmetry of C_{24} fullerene, Asian Journal of Chemistry, 20 (2008) 838-844.

[17] W. An, N. Shao, S. Bulusu, X.C. Zeng, Ab initio calculation of carbon clusters. II. Relative stabilities of fullerene and nonfullerene C24, Journal of Chemical Physics, 128 (2008).

[18] T. Oku, A. Nishiwaki, I. Narita, Formation and atomic structure of $B_{12}N_{12}$ nanocage clusters studied by mass spectrometry and cluster calculation, Science and Technology of Advanced Materials, 5 (2004) 635-638.

[19] M.T. Baei, M.R. Taghartapeh, E.T. Lemeski, A. Soltani, A computational study of adenine, uracil, and cytosine adsorption upon AlN and BN nano-cages, Physica B: Condensed Matter, 444 (2014) 6-13.

[20] H.-p. Chen, J.-n. Ding, N.-y. Yuan, X.-q. Wang, C.-l. Chen, D. Weng, First-principle study of interaction of H_2 and H_2O molecules with $(ZnO)_n$ (n=3–6) ring clusters, Progress in Natural Science: Materials International, 20 (2010) 30-37.

[21] M.T. Baei, A.A. Peyghan, Z. Bagheri, A DFT study on CO_2 interaction with a BN nano-cage, Bulletin of the Korean Chemical Society, 33 (2012) 3338-3342.

[22] A. Panahyab, H. Soleymanabadi, Ozone adsorption on a BN fullerene-like nano-cage: A DFT study, Main Group Chemistry, 15 (2016) 347-354.

[23] S. Munsif, K. Ayub, Permeability and storage ability of inorganic $X_{12}Y_{12}$ fullerenes for lithium atom and ion, Chemical Physics Letters, 698 (2018) 51-59.

[24] J.C. Escobar, M.S. Villanueva, A.B. Hernández, D. Cortés-Arriagada, E.C. Anota, Interactions of B12N12 fullerenes on graphene and boron nitride nanosheets: A DFT study, Journal of Molecular Graphics and Modelling, 86 (2019) 27-34.

[25] J. Beheshtian, I. Ravaei, Hydrogen storage by BeO nano-cage: A DFT study, Applied Surface Science, 368 (2016) 76-81.

[26] Y. Mo, H. Li, K. Zhou, X. Ma, Y. Guo, S. Wang, L. Li, Acetone adsorption to $(BeO)_{12}$, $(MgO)_{12}$ and $(ZnO)_{12}$ nanoparticles and their graphene composites: A density functional theory (DFT) study, Applied Surface Science, 469 (2019) 962-973.

[27] A. Soltani, A.S. Ghasemi, M.B. Javan, F. Ashrafi, J.C. Ince, F. Heidari, Adsorption of HCOH and H_2S molecules on $Al_{12}P_{12}$ fullerene: a DFT study, Adsorption, 25 (2019) 235-245.

[28] B. Wanno, V. Ruangpornvisuti, DFT investigation of structures of nitrosamine isomers and their transformations in gas phase, Journal of Molecular Structure: THEOCHEM, 766 (2006) 159-164.

[29] I.N. Levine, Quantum Chemistry, Pearson Education2013.

[30] T. Engel, P. Reid, Physical Chemistry, Pearson Education2012.

[31] C.J. Cramer, Essentials of Computational Chemistry: Theories and Models, Wiley2013.

[32] E.G. Lewars, Computational Chemistry: Introduction to the Theory and Applications of Molecular and Quantum Mechanics, Springer, Cham2016.

[33] J.W. Ochterski, Thermochemistry in Gaussian, Gaussian, Inc., (2000).

[34] A.E. Reed, L.A. Curtiss, F. Weinhold, Intermolecular interactions from a natural bond orbital, donor-acceptor viewpoint, Chemical Reviews, 88 (1988) 899-926.

[35] D.C. Young, Computational Chemistry: A Practical Guide for Applying Techniques to Real World Problems, John Wiley & Sons, Inc.2001.

[36] T. Yanai, D.P. Tew, N.C. Handy, A new hybrid exchange-correlation functional using the Coulomb-attenuating method (CAM-B3LYP), Chemical Physics Letters, 393 (2004) 51-57.

[37] A.D. Becke, Density-functional thermochemistry. III. The role of exact exchange, The Journal of Chemical Physics, 98 (1993) 5648-5652.

[38] C. Lee, W. Yang, R.G. Parr, Development of the Colle-Salvetti correlation-energy formula into a functional of the electron density, Physical Review B, 37 (1988) 785-789.

[39] W.J. Hehre, K. Ditchfield, J.A. Pople, Self-consistent molecular orbital methods. XII. Further extensions of gaussian-type basis sets for use in molecular orbital studies of organic molecules, The Journal of Chemical Physics, 56 (1972) 2257-2261.

[40] P.Y. Ayala, H.B. Schlegel, A combined method for determining reaction paths, minima, and transition state geometries, Journal of Chemical Physics, 107 (1997) 375-384.

[41] M.J. Frisch, et al., Gaussian 09, Revision D.01, Gaussian, Inc., Wallingford, CT, 2014.

[42] L.A. Curtiss, K. Raghavachari, P.C. Redfern, J.A. Pople, Assessment of Gaussian-2 and density functional theories for the computation of enthalpies of formation, Journal of Chemical Physics, 106 (1997) 1063-1079.

[43] J.W. Ochterski, G.A. Petersson, K.B. Wiberg, A Comparison of Model Chemistries, Journal of the American Chemical Society, 117 (1995) 11299-11308.

[44] J.O. Hirschfelder, E. Wigner, Some quantum-mechanical considerations in the theory of reactions involving an activation energy, The Journal of Chemical Physics, 7 (1939) 616-628.

[45] E. Wigner, On the quantum correction for thermodynamic equilibrium, Physical Review, 40 (1932) 749-759.

[46] S. Li, Semiconductor Physical Electronics, Springer, USA, 2006.

APPENDIX

Table S 1 The shortest bond–distances between atom(s) of nitrosamine conformers and surface atom(s) of CSL, BNSL, BeOSL and AlPSL nanocages.

Configuration	Mode [a,]	Bond [b,c]	Bond distance [d]
CSL:			
a–nsm/CSL–1	Diss Chem	N1···C1, N2···C2	1.49, 1.44
a–nsm/CSL–2	Phys, single mode	H1···C1	2.64
i–nsm/CSL–1	Chem	N1···C1, N2···C2	1.48, 1.46
i–nsm/CSL–2	Chem	N1···C1, N2···C2	1.49, 1.46
i–nsm/CSL–3	Phys, double mode	O···C1, N2···C2	3.50, 3.34
BNSL:			
a–nsm/BNSL–1	Chem	N1···B, H1···N	1.68, 2.06
a–nsm/BNSL–2	Chem	N1···B	1.67
a–nsm/BNSL–3	Chem	N2···B	1.69
a–nsm/BNSL–4	Phys	N1···N	2.13
a–nsm/BNSL–5	Chem	H1···N, H1···N	1.60, 1.68
i–nsm/BNSL–1	Chem	N1···B, H1···N	1.66, 1.72
i–nsm/BNSL–2	Chem	N1···B	1.65
i–nsm/BNSL–3	Chem	N1···B	1.67
i–nsm/BNSL–4	Chem	N1···B	1.66
i–nsm/BNSL–5	Chem	N1···B, H1···N	1.66, 1.80
i–nsm/BNSL–6	Chem	N1···B	1.67
i–nsm/BNSL–7	Chem	N2···B	1.62
i–nsm/BNSL–8	Chem	N2···B	1.62
i–nsm/BNSL–9	Chem	N2···B	1.63
BeOSL:			
a–nsm/BeOSL–1	Chem	N1···Be, H1···O	1.84, 2.04
a–nsm/BeOSL–2	Chem	N1···Be	1.83
a–nsm/BeOSL–3	Phys	N2···Be	1.90
a–nsm/BeOSL–4	Phys	H1···O	1.93
a–nsm/BeOSL–5	Chem	O···Be, H1···O	1.72, 1.68

i–nsm/BeOSL–1	Chem	N1···Be, H1···O	1.82, 1.70

Table S1 continued

i–nsm/BeOSL–2	Chem	N1···Be	1.81
i–nsm/BeOSL–3	Chem	N1···Be	1.83
i–nsm/BeOSL–4	Chem	N1···Be	1.82
i–nsm/BeOSL–5	Chem	N1···Be, H1···O	1.81, 1.78
i–nsm/BeOSL–6	Chem	N1···Be	1.83
i–nsm/BeOSL–7	Chem	N2···Be	1.80
i–nsm/BeOSL–8	Chem	N2···Be	1.80
i–nsm/BeOSL–9	Chem	N2···Be	1.81
AlPSL:			
a–nsm/AlPSL–1	Chem	N1···Al, H1···P	2.15, 2.51
a–nsm/AlPSL–2	Chem	N1···Al	2.14
a–nsm/AlPSL–3	Phys	N2···Al	2.18
a–nsm/AlPSL–4	Chem	O···Al, H1···P	1.97, 2.28
i–nsm/AlPSL–1	Chem	N1···Al, H1···P	2.14, 2.28
i–nsm/AlPSL–2	Chem	N1···Al	2.13
i–nsm/AlPSL–3	Chem	N1···Al	2.15
i–nsm/AlPSL–4	Chem	N1···Al	2.13
i–nsm/AlPSL–5	Chem	N1···Al, H1···P	2.13, 2.37
i–nsm/AlPSL–6	Chem	N1···Al	2.14
i–nsm/AlPSL–7	Chem	N2···Al	2.06
i–nsm/AlPSL–8	Chem	N2···Al	2.08
i–nsm/AlPSL–9	Chem	N2···Al	2.06
i–nsm/AlPSL–10	Chem	N2···Al	2.08

[a] Interacting mode assignment.

[b] Bond distance (A···S) between atom A of gas and atom S of nanocage surfaces.

[c] Atomic labels are defined in Fig. 3.1.

[d] In Å.

VITAE

My name is Monrada Petchmark. I was born on 10th August 1996. My address is 323 Ban Prao sub-district, Pa Phayom district, Phatthalung 93210, Thailand. I graduated from high school at Phatthalung Scool in 2015. I have studied in Bachelor's degree of Science, Chulalongkorn University during 2015 – 2018. My contact is monrada.pet@gmail.com.